Journal Pre-proof

A Theoretical Framework for Evolutionary Cell Biology

Michael Lynch, Bogi Trickovic

PII: S0022-2836(20)30156-X

DOI: https://doi.org/10.1016/j.jmb.2020.02.006

Reference: YJMBI 66445

To appear in: *Journal of Molecular Biology*

Received Date: 29 October 2019

Revised Date: 20 January 2020

Accepted Date: 4 February 2020

Please cite this article as: M. Lynch, B. Trickovic, A Theoretical Framework for Evolutionary Cell Biology, *Journal of Molecular Biology*, https://doi.org/10.1016/j.jmb.2020.02.006.

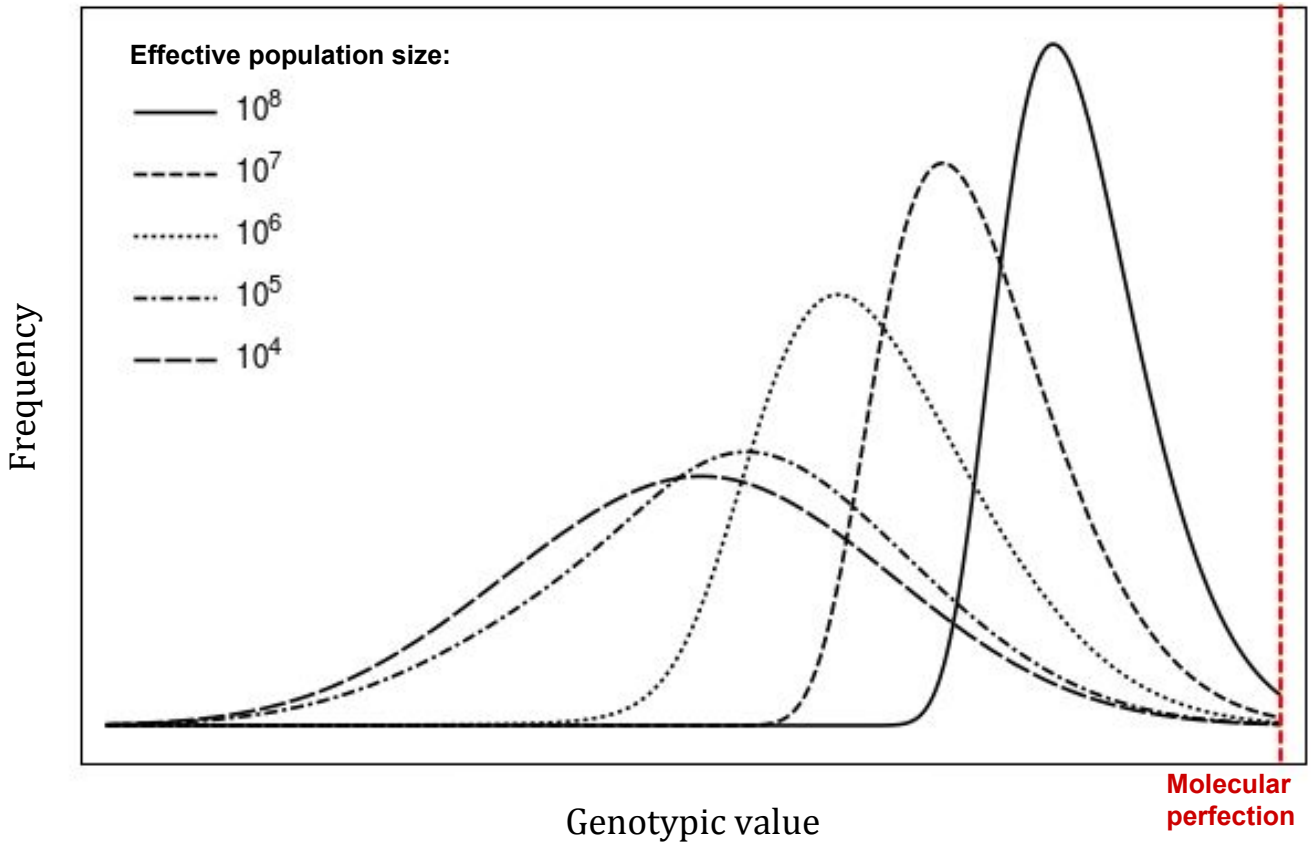
Effective population size:
10^8
10^7
10^6
10^5
10^4
Frequency
Genotypic value
Molecular perfection

A Theoretical Framework for Evolutionary Cell Biology

Michael Lynch and Bogi Trickovic

Biodesign Center for Mechanisms of Evolution, Arizona State University, Tempe, AZ 85287
mlynch11@asu.edu

Abstract

One of the last uncharted territories in evolutionary biology concerns the link with cell biology. Because all phenotypes ultimately derive from events at the cellular level, this connection is essential to building a mechanism-based theory of evolution. Given the impressive developments in cell biological methodologies at the structural and functional levels, the potential for rapid progress is great. The primary challenge for theory development is the establishment of a quantitative framework that transcends species boundaries. Two approaches to the problem are presented here: establishing the long-term steady-state distribution of mean phenotypes under specific regimes of mutation, selection, and drift; and evaluating the energetic costs of cellular structures and functions. Although not meant to be the final word, these theoretical platforms harbor potential for generating insight into a diversity of unsolved problems, ranging from genome structure to cellular architecture to aspects of motility in organisms across the Tree of Life.

All organismal features are functions of structures and processes that develop at the cellular level. Thus, given that most of the prominent advances in the life sciences over the past fifty years have emerged from the field of cell biology, the incorporation of cell-biological issues into the mainstream of evolutionary science is long overdue [1]. Establishing a formal field of evolutionary cell biology will have to integrate the cataloging of diversity via comparative studies into an explanatory theoretical framework. The goal is not to simply document what has evolved, but to understand the mechanisms by which change has come about and might be encouraged (or discouraged) from proceeding in certain practical situations.

Developing such theory is challenging, as there is a need for a conceptual framework for testing alternative evolutionary hypotheses. Unlike the situation in the well-trodden fields of molecular and genomic evolution, the subject matter is not a linear readout of nucleotides or amino acids. One cannot construct a neutral (null) evolutionary hypothesis for variation in a cellular trait based on the expected behavior in the absence of selection and then contrast this with observed trait values (a strategy widely embraced in molecular-evolution studies that compare, for example, silent and amino-acid replacement sites in protein coding genes). The problem here is that most cellular features involve complexes of multiple types of organic molecules (nucleic acids, proteins, lipids, and carbohydrate derivatives) and/or dynamic reaction rates that depend on the cellular environment, sometimes with the key components changing among phylogenetic lineages.

In exploring some potential paths forward, we start with the general assumption of uniformitarianism. That is, as with the laws of physics and chemistry, we assume that the general mechanisms of evolution observed today have applied across the Tree of Life for the past three billion or so years in which cells have occupied the planet. By extension, we assume that these mechanisms are consistent with the basic principles of evolutionary population genetics that have been laid down over the past century of research [2,3]. Based on a myriad of empirical observations on the genetics and stochastic features of inheritance, mutation, and recombination, combined with the ubiquitous force of natural selection, the field of population genetics is now so well-established that any credible evolutionary framework needs to either be fully consistent with evolutionary-genetic principles or to explain why a perceived deviation from such principles remains in the realm of rational discourse.

As an entrée to developing a theoretical foundation for evolutionary cell biology, we propose two potential approaches that can be readily integrated into a hypothesis-testing framework. As these are early days for this field, alternative points of view are desirable. One of the most significant problems in the broader body of biological thinking is the common assumption that all observed aspects of biodiversity are products of natural selection [4,5]. With this mind set, evolutionary biology becomes little more than a (sometimes endless) exercise in dreaming up the supposed agents of selection molding one's favorite aspect of phenotypic diversity. However, we now know that this unwavering belief in the limitless power of natural selection is untenable. For example, much of the substantial molecular/genomic variation across the Tree of Life can only be understood by appreciating the inability of natural selection to oppose certain kinds of mutational changes [6–8].

One might be inclined to believe that as the focus expands to higher-level aspects of cellular organization, the likelihood of anything other than natural selection dictating the course of evolution will become diminishingly small. As will be demonstrated below, however, there is now substantial evidence that stochastic forces due to finite population size and chromosome structure always dictate what natural selection can and cannot promote/oppose in alternative phylogenetic contexts. This means that a rational field of evolutionary cell biology will require some resistance to the seduction of adaptive story telling. It remains true that evolution is a process of descent with modification, and few traits are overtly maladaptive, but the processes that enabled the emergence of certain attributes millenia ago need not reflect current-day functions.

As we hope to reach a broad audience, we start with an outline of the basic principles of population genetics essential to understanding the limits to what natural selection can accomplish, with particular emphasis on how the forces of mutation and random genetic drift conspire to define the bounds within which mean phenotypes of traits are likely to wander over evolutionary time. We next explore how results from the fields of bioenergetics and biochemistry provide one particular approach to integrating the vast array of results from molecular cell biology with evolutionary theory. After considering applications of these ideas to an array of issues in cell biology, we close with a discussion of the plausibility of the idea that many aspects of cellular diversity, particularly in eukaryotes, have been channeled by nonadaptive forces of evolution, calling into question the common view that eukaryotes are on a progressive evolutionary march towards adaptive perfection.

The Population-genetic Environment and the Limits to Natural Selection

Evolution is a dynamical process that sometimes reaches equilibrium states when there is a balance between opposing forces of allele-frequency change (e.g., mutation and selection biases operating in opposite directions). One of the lessons learned from decades of genetic surveys at the DNA level is that, at any one time, there are typically no more than one or two nucleotide variants simultaneously present at the same genomic site within a population. This simplifies many aspects of theoretical population genetics [3]. If p is the frequency of a particular variant at a nucleotide site, and s is its selective advantage (or disadvantage), the expected change in allele frequency across generations is $sp(1-p)$, where $p(1-p)$ is a measure of variation at this site (equivalent to half the heterozygosity under random mating). Variants of this expression exist if there are nonadditive interactions among alleles, but this will not qualitatively alter the general points to be made below.

Of special relevance is the fact that $sp(1-p)$ is the *expected* rate of allele-frequency change in the absence of opposing forces. If the latter conditions are met, a beneficial allele will simply march to fixation (frequency $p = 1$). However, except in rare cases of extraordinarily strong selection, one or more opposing forces almost always influence the fates of mutant alleles. One of the key determinants of allele-frequency change is random genetic drift, which we define here as the cumulative effect of various sources of noise in the gene-transmission process across generations, subsumed into a parameter called the genetic effective population size N_e [9]. Notably, genetic drift operates like a diffusion process, with the variance in allele-frequency change across generations being equal to $p(1-p)/N_e$. (The denominator must be multiplied by two in a diploid population, but we will adhere to a haploid situation throughout).

Because both the change in allele-frequency via selection and the variance in allele-frequency change via drift are proportional to $p(1-p)$, the ratio $s/(1/N_e) = N_e s$ is a general indicator of the ratio of the power of selection to drift, independent of allele frequency. This benchmark proves to be central to many aspects of molecular, genomic, and cellular evolution [3,10]. For situations in which $N_e|s| \gg 1$, selection is the primary determinant of the fates of common alleles (although drift always plays a role at low frequencies). If, however, $N_e|s| \ll 1$, natural selection is rendered powerless, as the stochastic forces of drift always overwhelm the deterministic force of selection, a condition called effective neutrality. The key point is that as N_e declines, the fraction of mutations (beneficial and deleterious) with fates largely determined by drift necessarily expands.

Many factors influence the genetic effective size of a population [3, 9, 11]. In the ideal case in which family sizes are random, N_e is simply equal to the number of reproductive adults, N_a. However, most demographic factors conspire to make N_e smaller than N_a, often by orders of magnitude – due to environmental heterogeneity, family sizes are generally not random; sex ratios can deviate from 1:1; and temporal bottlenecks in N_a have much more long-lasting effects than do population-size expansions. More importantly, however, many aspects of the stochastic transmission of allele frequencies across generations are due to intrinsic genetic factors rather than to demographic forces.

Most mutations are detrimental to fitness, creating a background of low-frequency deleterious alleles distributed across chromosomes and individuals in all populations. As a consequence, a new beneficial mutation will frequently arise at a location closely linked to deleterious variants at other sites, reducing its net selective advantage, in some cases to the point of being dragged out of the population by negative selection against the linked variants, a process known as background selection [9]. The magnitude of this force depends on the rate of recombination, which can liberate a beneficial allele from its deleterious background. However, even when a beneficial mutation appears on a clean genetic background, it can become a victim of newly arising linked deleterious background mutations. Moreover, selective interference also occurs between beneficial mutations at different genomic locations, as these simultaneously compete for fixation. The key point is that even extremely large populations can be subject to relatively strong stochastic effects, with reduced N_e being primarily a consequence of genes being linked together on chromosomes. In very large populations, N_e is expected to scale very slowly (approximately logarithmically) with N_a [12].

Negative scaling of the effective population size with organism size. One of the central empirical challenges in evolutionary biology is acquiring estimates of N_e. Ideally, N_e would be measured directly from temporal fluctuations in allele frequencies, but this is essentially impossible for very large populations, as the true fluctuations are so small as to be unobservable with reasonable sample sizes and time scales. An alternative approach relies on observed population levels of variation at nucleotide sites assumed to be largely free of the forces of selection (e.g., silent sites at the third positions of codons). Under long-term drift-mutation equilibrium, the average level of nucleotide variation at such sites (here defined to be the mean heterozygosity between randomly paired gametes or haploid genomes) is equal to the ratio of the power of mutation to that of drift, $2N_e u$, where u is the mutation rate per nucleotide site per generation (the 2 being replaced by 4 in diploids). When a measure of such variation is

available along with an estimate of the mutation rate, N_e can be estimated by factoring out $2u$.

As a large number of direct estimates of u are now available to a high degree of precision (below), some general statements can be made about estimates of N_e obtained in this way. First, over a 17 order-of-magnitude gradient of organism size (mass per adult) across the Tree of Life, there is a progressive, nearly three order-of-magnitude decline in N_e (Lynch et al., submitted) (Figure 1). Large vertebrates typically have N_e in the range of 10^4 to 4×10^5, invertebrates in the range of 3×10^5 to 3×10^6, and vascular plants have N_e intermediate to these two groups. On the other hand, N_e in microbial eukaryotes ranges from 4×10^6 to 2×10^8. Bacteria have still higher N_e, but in no case does this exceed 5×10^8. As a pile of 10^9 bacterial cells occupies ~ 1 mm^3, these results make clear that N_e is typically many orders of magnitude smaller than the absolute population size.

These observations imply that the pool of mutations available to natural selection is potentially much broader in microbes than in multicellular species. Recalling the approximate breakpoint for effective neutrality, $|s| < 1/N_e$, natural selection in bacteria can perceive mutations with absolute effects as small as 10^{-9}, whereas the critical cutoff in vertebrates is more on the order of $s = 10^{-5}$. This four order-of-magnitude gradient of critical s implies that natural selection has the capacity to exploit much more fine-scale variation in bacteria than is the case in eukaryotes, particularly in multicellular species.

The molecular resource base for natural selection. The degree to which this gradient in the drift barrier translates into differential susceptibility to adaptive evolution ultimately depends on the distribution of fitness effects of new mutations. For random genetic drift to impose a significant barrier to the evolutionary refinement of a trait, there must be a substantial pool of deleterious mutations with small enough effects that they can drift to fixation in species with small N_e. Although it is difficult to make statements about specific cellular traits, numerous lines of evidence suggest that the vast majority of mutations have deleterious effects, with the distributions of fitness effects associated with both beneficial and deleterious mutations being biased to near-zero values.

First, serially bottlenecked mutation-accumulation (MA) lines across diverse species, designed to specifically prevent the influence of selection on the pool of *de novo* mutations, consistently reveal a slow per-generation decline in growth rate and other fitness-related traits, as expected with a strong predominance of mutations with deleterious effects [13, 14]. Second, statistical inferences based on the performance of individual MA lines imply highly skewed distributions of fitness effects, with the modes for both deleterious and beneficial effects indistinguishable from zero, and the bulk of the distributions having absolute effects below 1% [15–17]. Third, more indirect details on the mutational distribution of fitness effects, derived from studies on the site-frequency spectra of segregating alleles, commonly suggest that 10 to 40% of mutations in diverse organisms have deleterious effects smaller than 10^{-5}, with the mode of this pool again being near (if not at) 0.0 [18–22]. Fourth, bioenergetic considerations of the costs of small nucleotide insertions, which typically comprise $\sim 10\%$ of *de novo* mutations [23], imply fractional reductions in fitness typically far below 10^{-4} per mutation [8]. Thus, the existence of large pools of mutations with effects small enough to be immune to selection in some lineages but large enough to ensure removal/promotion by selection in others is not in doubt.

The Drift Barrier to Cellular Perfection

The substantial contributions of mutations of small effect to phenotypic variation and fitness raise questions about the common view that all aspects of cell biology are fine-tuned by the unlimited power of natural selection. To further clarify several points, we introduce a simple model to illustrate how the mean phenotype of a complex trait is expected to respond to the joint forces of selection, mutation, and random genetic drift. The starting point is the assumption that the intensities and patterns of these forces remain relatively constant over a long period. Under such a scenario, stochastically arising mutations have a certain probability of being promoted by selection and/or simply drifting to fixation, and back mutations ensure that movement in the opposite direction can also occur. Over a long evolutionary time period, the mean phenotype will then wander within a range dictated by the prevailing forces of selection and the diffusive properties of mutation and random genetic drift. As a result, there is not a single point equilibrium, but rather a quasi-steady-state distribution of mean phenotypes, which can be viewed as the temporal distribution of mean phenotypes over time for a particular lineage or as the dispersion of isolated lineages experiencing the same population-genetic environment. Although this type of model may be viewed as unrealistic for evolutionary responses to temporally varying ecological changes, it serves as a reasonable heuristic guide to the evolution of intracellular features carrying out conserved functions for eons in settings buffered by internal homeostatic mechanisms.

Consider a trait for which the genotypic value is determined by ℓ genetic loci (or nucleotide sites) each having two

possible allelic states (+ or −) with additive effects, and with the rate of mutation from + to −, and the reverse, being u_{10} and u_{01}, respectively. Although there are 2^ℓ possible haplotypes, because of the equivalence of effects across all loci, there are only $(\ell+1)$ genotypic values (defined by the number of + alleles) (Figure 2). If the population size is suitably small (such that the expected number of mutations arising in the population per generation for the trait is < 1), evolution will proceed in an essentially stepwise manner between adjacent classes. With paths connecting all adjacent states, complete exploration of genotypic space is possible.

Under this model, the rates of transition between states depend on the products of mutation rates and probabilities of fixation of newly arising mutations. The former depends on the genotypic state (number of +/− alleles) and the population size, whereas the latter is described by Kimura's equation [24], which depends on N_a, N_e, and s. This model has already been applied to cell biological features such as transcription factors and their binding sites [1] and the alternative states of multimeric proteins in [25]. The goal here is simply to make the interpretation of the theoretical results more transparent.

A useful feature of the linear mutation model is that the equilibrium probability of each genotypic state m is simply equal to the product of the transition rates on the arrows pointing toward the state from above and below, with the final result condensing to

$$\tilde{p}_m = C \cdot p_m^* \cdot e^{2N_e s_m} \tag{1a}$$

C is the normalization constant, equal to the reciprocal of the sum of the terms to the right of C for $m = 0$ to ℓ, which scales the sum of probabilities to 1 [26]. The coefficient s_m is a measure of the selective advantage of genotypic class m relative to some reference point (usually scaling the most fit class to have fitness 1.0 and all other classes to have relative selective disadvantages $s_m < 0$). The quantity $N_e s_m$ is then equivalent to the now familiar ratio of the strength of selection relative to drift for genotypic class m. Finally,

$$p_m^* = \binom{\ell}{m} \eta^m (1-\eta)^{\ell-m} \tag{1b}$$

is the expected distribution of genotypic values under neutrality (were drift and mutation to be the only evolutionary forces), equivalent to the binomial distribution, with $\eta = u_{01}/(u_{01}+u_{10})$ being the expected frequency of + alleles at each site in this case. Taken together, Equations (1a,b) show that the steady-state probability distribution under selection is a simple multiplicative transformation of the neutral expectation, with the weight for each class being the exponential function of the scaled strength of selection, $e^{2N_e s_m}$. Under neutrality, $s_m = 0$ for all m, reducing Equation (1a) to (1b). The mean equilibrium value of m, $\mu_D = \sum \tilde{p}_m \cdot m$, is the drift barrier – mean phenotypes that are closer to a local optimum than μ_D might transiently arise by mutation but cannot be sustained, owing to the inefficiency of selection beyond such a point.

The evolutionary implications of this model can be summarized as follows. First, Equations (1a,b) make clear the role of mutation bias in evolution, a subject of recent debate [27–30]. The steady-state genotype distribution depends only on the distribution of mutational effects, i.e., on the ratio of mutation rates, not on the mutation rate itself. Moreover, mutation bias alone does not simply push the genotype distribution to a particular location in the absence of selection. Rather, the multiplicity of haplotypes within genotypic classes is a strong determinant of the mean of the distribution. In the absence of selection, the genotypic mean is $\ell\eta$ (the expected number of + alleles per genome), and with increasing N_e natural selection progressively pushes the distribution towards the optimum value. This means that depending on the number of loci involved (ℓ) and the position of the optimum, the location of the mean phenotype (genotypic value) can either increase or decrease with increasing N_e. The central point is that, even in the absence of mutation bias, the multiplicity of functionally equivalent haplotypic states acts as an evolutionary attractor, ensuring that the mean phenotypes of complex traits will almost never perfectly coincide with optima defined by natural selection.

Second, even though natural selection can efficiently move the expected genotypic means toward the optimum with increasing N_e, there can still be considerable variance in the distribution. This can be seen in the example given in Figure 3, where there is persistent directional selection towards the highest genotypic value; other examples with alternative fitness functions can be found in [1, 26]. The exact scaling of the overall mean phenotype with N_e will depend on the form of the fitness function, but the standard deviations of the steady-state distributions are often on the order of 20% or so of the mean. The central point here is that the stochastic forces of drift and mutation cause population mean phenotypes to wander around the drift barrier. This behavior should be of concern to those who

wish to interpret all of interspecific variation in mean phenotypes as inevitable outcomes of natural selection.

We close this section with two examples that seem to be in accordance with the drift-barrier hypothesis. First, one of the only cellular traits for which there is a broad set of estimates across the Tree of Life is the mutation rate per nucleotide site per generation (u) [31, 32]. Because the vast majority of mutations are deleterious, theory suggests that mutator alleles are generally selected against as an indirect consequence of the linked load of deleterious mutations that they promote [33, 34]. This is a relatively weak form of selection because the excess load associated with a mutator allele is equal to the genome-wide deleterious mutation rate itself, some of which is removed by recombination. Such a load will become progressively smaller as the mutation rate is reduced by selection in populations with larger N_e, as the maximum improvement cannot exceed that which would be accomplished by complete replication fidelity.

Consistent with a drift-imposed gradient, there is a negative scaling of the mutation rate over a five order-of-magnitude increase in N_e (Figure 4). Although the quantitative scaling varies among groups of organisms, this too is consistent with the theory. For example, the five- to ten-fold reduction in u in unicellular eukaryotes relative to that in bacteria is in accordance with the idea that the magnitude of selection operating on the mutation rate is a function of the genome-wide deleterious mutation rate summed over all functional sites [31], as eukaryotes have substantially more genomic material under selection than do bacteria (owing to the increase in gene number and regulatory DNA). Also consistent with the drift-barrier hypothesis for replication fidelity is the high mutation rate associated with "error-prone" polymerases involved in relatively small numbers of nucleotide transactions per cell cycle [35], and the substantial increase in transcript error rates, as their effects are transient over the life span of a cell [36, 37].

Second, as an illustration of the notion of multiplicity of alternative, functionally equivalent sites, consider the observations that have been made on post-translational modification in eukaryotes. Phosphorylation of amino-acid residues commonly plays a role in modifying protein activity, and comparative studies in yeasts and mammals indicate that many phosphorylated serines and threonines are under purifying selection to retain their phosphosite status [38–41]. However, large fractions of phosphosites appear free to vary among species in terms of status and location [42–45]. For example, only $\sim 5\%$ of all *S. cerevisiae* phosphorylation sites are conserved across the entire yeast lineage (dating back ~ 700 million years), and even when the same phosphorylatable residue is present in two moderately related species, their phosphorylation status may differ. In addition, Asp and Glu residues, which are naturally charged negatively, serve as potential replacements for their phosphorylatable counterparts, i.e., phosphosites often evolve from phosphomimetic Asp and Glu sites and vice versa [46–48]. Taken together, these observations suggest a scenario whereby the number of phosphorylated residues on individual proteins behaves like a quantitative trait under stabilizing selection for an appropriate negative charge (with site-specific digital properties, like those represented in Figure 2), but with enough degrees of freedom that the specific locations of the affected residues are free to wander in an effectively neutral fashion [49, 50].

For purposes of presentation, the model presented above has been idealized in a number of ways. For example, mutations with a distribution of effects have not been included, and the model assumes that evolutionary transitions move from one essentially fixed state to another adjacent state, ignoring the possibility of vaulting multiple states in populations with very large N_e. Although implementation of these modifications into the theory is desirable, violations of these assumptions are unlikely to alter the qualitative conclusion that the level of achievable cellular perfection will scale with N_e. Allowing for a distribution of mutational effects should strengthen this conclusion, as it will extend the range of effective neutrality for a subset of mutations into a larger range of N_e. For traits involving a very large number of loci, such as growth rate, the elevated gradient in multiplicity is expected to play a more substantial role in causing a trait to stabilize at positions below the optimum.

The Bioenergetic Constraints on Cellular Evolution

The proposed explanation for the negative scaling of the mutation rate with N_e is based on population-genetic theory defining the average linked fitness burden of mutator genotypes that builds up over hundreds of generations of mutation accumulation. However, most cellular modifications have immediate impacts via impacts on the cell's energy budget resulting from the synthesis of the basic building blocks for trait construction. Unless the fitness advantages provided by the trait modification outweigh the investment costs by an amount exceeding the power of drift, promotion by natural selection is not possible, although if effectively neutral, the variant may drift to fixation and may even be driven towards that end by mutation bias.

At the heart of this subject are two central concepts in biology: 1) the costs of building and maintaining cellular

features and any resultant benefits in terms of biomass production; and 2) the degree to which such alterations translate into fitness differences influencing long-term evolutionary trajectories. Here, we attempt to sketch out a quantitative framework for addressing these issues, following the procedures outlined in [8] and [51].

The bioenergetic cost of a cellular feature. As with others before us [52–56], for practical reasons, we will quantify costs in units of ATP hydrolyses (or their equivalent), the universal currency of bioenergetics across the Tree of Life. Situations do exist in which energy is not the limiting resource, e.g., phytoplankton populations with some key element such as carbon, nitrogen, phosphorus, or a trace metal constraining the rate of cell growth. For microbes growing on a defined medium with a single compound providing carbon and energy (and all other nutrients in excess supply), the growth yield per carbon consumed increases linearly with the substrate heat of combustion (which is linearly related to the number of C-H bonds available for oxidation; [57] up until a threshold value, thereafter leveling off (Figure 5). This suggests that below a critical value of $\simeq 10$ kcal/g resource carbon, growth for most heterotrophs is limited by energy, whereas above this threshold the food supply contains excess energy relative to carbon content required for growth. Notably, the most common substrate used in microbial growth experiments, glucose, has a heat of combustion of 9.3 kcal/g carbon, close to the threshold at which growth is equally limited by carbon and energy.

Although cases involving non-energy limitation may require a shift in the currency to be used, the conceptual framework outlined below should still apply. Regardless of the substrates being consumed, all aspects of cellular maintenance and growth require energy, and although the yields of microbes grown on alternative substrates (per unit carbon consumed) vary with the nature of the substrate (Figure 5), few commonly used substrates have yields more than 50% below the threshold value, and the estimated numbers of ATP hydrolyses necessary to build an offspring cell are relatively independent of the substrate employed [52, 55, 56]. This provides at least partial justification for using ATP as the currency in the kinds of computations outlined below.

In evaluating the total cost of a cellular feature, four categories of investment must be considered (Figure 6). First, nearly all cellular features are assembled from four types of monomeric building blocks – amino acids, nucleotides, lipid molecules, and/or carbohydrates, which if not acquired externally, must be synthesized by processes requiring carbon skeletons and energy investments, e.g., from transformations of glucose or acetate to precursor metabolites that are then further processed. Second, the construction of a higher-order structure from its basic building blocks imposes assembly costs, such as expenditures in polymerizing nucleic-acid and amino-acid chains, adding post-translational modifications, etc. Third, the maintenance of biomolecules generally imposes still additional costs such as accommodation of molecular turnover. Although there are acquisition costs for obtaining external resources, e.g., use membrane-bound channels, phagocytosis, and mobility, these occur upstream of the steps used in trait construction/maintenance and are not considered in the following analyses.

Finally, in addition to the three sets of direct costs of constructing and maintaining a trait, there will usually be indirect costs associated with diverting resources that would otherwise be available for other cellular functions (Figure 6). Such costs are incurred because metabolic precursors used in the biosynthesis of the building blocks of the trait under consideration can no longer be used for ATP production or as carbon skeletons for other structures. Atkinson defined these secondary, opportunity costs as the "prices of metabolites," [53] and seemingly independent of him, Craig and Weber and Akashi and Gojobori used this approach to partition the costs of amino acids into components associated with the investment in synthesis and the diversion of metabolic precursors [58, 59].

To sum up, the total cost of constructing and maintaining a trait and diverting components from alternative usage to do so is the sum of the direct and opportunity costs over the entire lifespan of the cell,

$$c_T = c_D + c_O \tag{2}$$

Whereas c_D will be reflected in ATP hydrolysis reactions leading to heat dissipation (owing to imperfect exploitation of energy release), opportunity costs do not generate heat, as ATP is not consumed.

Given the near universality of many biosynthetic pathways and enzyme-reaction mechanisms across the Tree of Life, this general approach holds promise, as the steps for calculating most costs can often be gleaned from information in the literature [8, 51]. The biosynthetic costs of the basic monomeric building blocks are on most solid footing. For example, although there is variation among residues, the average direct and opportunity costs per amino acid are ~ 2 and 25 ATP hydrolyses [51]. There is little variation in costs among nucleotides, the average being ~ 11 and 34 ATPs for DNA and 10 and 31 ATPs for RNA for the direct and opportunity costs, respectively. The costs of lipids are much higher – although there is variation among lipid types depending on the fatty-acid chain length and

the number of unsaturated carbons, as a first-order approximation the average total cost per lipid molecule is ~ 425 ATP equivalents, approximately one-third of which involves direct cost [22].

The evolutionary cost of a cellular feature. Given a measure of the total energetic cost of a cellular feature (or modification thereof), the evolutionary implications revolve around three issues: 1) use of an appropriate definition of the cost from the perspective of organismal fitness; 2) scaling of this cost relative to the total cost of building and maintaining the cell; and 3) conversion of the appropriately scaled measure to a fitness differential.

First, although we have defined c_T in terms of direct and opportunity components, the latter will not always influence cellular performance. Consider, for example, an organism experiencing a saturating carbon/energy source but limited by a micronutrient such as iron. If the energy extracted from the food source is in excess supply and therefore under-utilized, the appropriate energetic cost from a fitness perspective is simply $c_T \simeq c_D$.

Second, supposing the cell has a baseline total energy budget per cell cycle of C_T (including the costs of both growth and maintenance; [8], the presence of the trait under consideration alters the lifetime energy budget to $C_T' = C_T + c_T$. Note that our view here is that C_T is the sum of direct and opportunity costs, which includes the direct energetic expenditure of ATP on biosynthesis and the indirect diversion of energy-containing carbon skeletons (opportunity loss), as would be reflected in the consumption of glucose molecules consumed in a chemostat and their conversion to ATP equivalents. If the cell-division time is τ in the absence of the trait, this additional investment in the trait will alter the cell-division time to $\tau' > \tau$ (for the time being ignoring any downstream fitness benefits, as the goal is to understand the baseline investment costs).

Finally, to understand the total bioenergetic investment in a trait from a fitness perspective, we need to define its effects on the cell's reproductive output relative to that in the absence of such an excess investment. Previous work intuited that the intrinsic selective disadvantage of any cellular feature is proportional to the fraction of the total energy pool per cell lifetime used up by the putative structure [8]. More precisely, the selective disadvantage s_c of a cellular feature is defined as the rate of offspring production by a mutant containing the feature (with the total cost c_T) relative to that of the "wild-type" without such a feature. Thus, for every wild-type offspring, there will be on average $1 - s_c$ mutant offspring. Recent theoretical work justified such intuition [60], except that a correcting factor of $\ln(R)$ is required, where R is the mean number of offspring produced per individual per generation. In the case of binary fission, $R = 2$, yielding

$$s_c \simeq \frac{\ln(2) \cdot c_T}{C_T} \tag{3}$$

For organisms experiencing variable environments, s_c might change substantially across generations owing to shifts in the numerator and/or denominator of this expression, and for a clonally reproducing organism this might be accommodated by evaluating geometric mean fitness.

The key parameter in this expression is the total energy budget of a cell, C_T. There are a number of ways to obtain this, one of the most powerful being the method of Pirt [61], which requires growth of the study organism at different dilution rates in a chemostat – the slope of a plot of the rate of resource consumption vs. the dilution rate (equivalent to the cell-division rate) provides a direct estimate of the amount of resource consumption per cell division, whereas the intercept estimates the basal (time-dependent) rate of investment in maintenance. Generally, in applications of this method a single compounds, such as glucose, as the sole source of carbon skeletons and energy. Given a knowledge of fraction of carbon incorporated into biomass, the metabolic pathway(s) utilized, and known conversion factors, these measures can then be transformed into units of ATP utilization. Summarizing results from a wide variety of organisms, Lynch and Marinov (2015) found that the total energy required to build a cell scales isometrically with cell volume (across both bacteria and eukaryotes). These results can be applied to Equation (5) as a first-order approximation in the absence of direct observations of C_T on a study organism.

One caveat with respect to the preceding derivation is that it focuses entirely on the bioenergetic costs of producing a trait. In some cases, there may be additional side effects, as when a novel protein promiscuously interacts with inappropriate substrates and/or excessively occupies cellular volume or membrane real estate in ways that negatively impinge on r. Because the total fitness cost of a cellular addition is in most cases likely to be so small as to be beyond the reach of experimentation, separating these indirect effects from the more immediate bioenergetic costs

may only be possible by computational analysis.

Finally, we note that an alternative route to estimating evolutionary costs may reside in the more systems-biology approach introduced by Molenaar and collaborators [62] and elaborated by others [63–65]. Here, the idea is that the internal biochemistry of the cell can be represented by a small number of mutually constrained molecular categories (e.g., ribosomes, nutrient acquisition, and all others), with the growth rate emerging as a function of the allocation of proteome to these different pools. In this context, a novel cellular feature could be viewed as competing energetically for resources allocated the pre-existing pools, and indeed this framework has already been used to explore the growth impediment owing to expression of a useless protein [63] or the insertion of a synthetic circuit [64]. It remains to be seen whether this conceptual framework, developed for *E. coli,* is generalizable to other species, and as the tradeoff constraint employed is conceptually similar to the opportunity costs invoked above, it is possible that both approaches will yield qualitatively similar results.

Applications to Cell Biological Traits

With the basic theory in place, the selective consequences of modifying, eliminating, or recruiting *in toto* (by, for example, horizontal transfer) any cellular feature can be evaluated provided certain information is available: 1) the energetic (or elemental) cost of the alteration; 2) the entire cost of building and maintaining the cell, which serves as a scaling factor for the former; and 3) the effective population size, which dictates the minimum relative cost that can be perceived by natural selection.

The general conceptual framework is outlined in Figure 7. Ignoring the bioenergetic cost, a particular cellular feature may appear to endow an organism with increased fitness owing to its affects on performance in response to a range of ecological challenges. However, in order for the feature to be promoted by selection, the benefits accrued must sufficiently offset the costs of producing and maintaining the trait to a significant enough extent that the net selective advantage exceeds the power of random genetic drift. If this is not the case, the feature will be subject to loss by deactivating mutations.

We now consider applications of the theory to some central issues in evolutionary cell biology, ranging from the genomic to the whole-organism level. With a goal of motivating further research, these examples merely outline the general issues, and there is ample room for further attention to technical details and extension to a diversity of organisms.

Gene and genome architecture. One of the clearest findings of the genomics era is the dramatic expansion of genome size and complexity from prokaryotes to unicellular eukaryotes to multicellular species [7]. Most of this inflation involves the addition of noncoding intergenic and intronic DNA. As natural selection places a premium on efficient resource utilization and reproduction in all species, how can this phylogenetic gradient in the expansion of nonfunctional DNA be explained? Accounting for the various biosynthetic, assembly, and maintenance costs, Lynch and Marinov found that most genes in *E. coli* have costs (summed over the DNA, mRNA, and protein levels) well above the drift barrier for this species (i.e., $s_c < 1/N_e \simeq 10^{-9}$) [8]. If, for example, one considers an insertion of just ten unexpressed nucleotides of double-stranded DNA, the total cost would be ~ 900 ATP hydrolyses (not including small additional processing costs associated with polymerization). Given that the total cost of building an *E. coli* cell is $\sim 3 \times 10^{10}$ ATPs, this means that the selective disadvantage of a functionally irrelevant 10-bp insertion of DNA is $\sim 3 \times 10^{-8}$, enough to be perceived by natural selection in this species.

Proceeding to yeast and then to multicellular species (*Arabidopsis* and humans), the absolute costs per gene (c_T) increase, owing to the increased investment in introns, untranslated flanking regions, histones, and substantially higher numbers of mRNAs and proteins expressed per cell. However, with an increase in cell volume, the total cost of building cells (C_T) increases 100- to 1000-fold up this gradient of organismal complexity, while the effective population size declines, lowering the drift barrier by factors of 10 to 1000 (Figure 1). This results in the progressive repositioning of the costs of most genes relative to the drift barrier, such that insertions of noncoding DNA as long as 10 to 100 kb are nearly invisible to the eyes of natural selection. These observations provide a more formal view of the commonly invoked "genomic streamlining" hypothesis. Because of their enormous N_e, bacteria are subject to the efficient removal of DNA that does not pay its way in terms of a significant selective advantage. In contrast, although selection still opposes genomic bloating with nonfunctional DNA in eukaryotes, drift is powerful enough to render such selection ineffective.

These same general principles can be applied to another aspect of genome and proteome structure that has attracted

considerable attention – the idea that the elemental composition of nucleic acids and proteins (e.g., C, N, P, and S content) is adaptively tuned to environmental conditions. Under this view, organisms living in environments depleted for a particular element are expected to evolve towards under-utilization of the same element in their nucelotide and amino-acid repertoires, and pathways involved in the metabolism of a scarce element are expected to evolve to avoid the inclusion of the same element in their infrastructure for acquiring said nutrient [66–68]. The advantages of such shifts at the level of single nucleotides or amino acids cannot be large, raising the question as to whether the population-genetic conditions necessary for the promotion of such modifications by natural selection are likely to be met. Here, it becomes necessary to measure costs in units of elemental composition rather than ATP equivalents.

Consider the use of carbon and nitrogen in nucleotides and amino acids. Over a range of growth conditions, the dry weight of *E. coli* cells consists of 45 to 47% carbon and 10 to 13% nitrogen [69]. The dry weight of an average cell in this species is ~ 0.00038 ng, implying $\sim 9 \times 10^9$ C and $\sim 2 \times 10^9$ N atoms per cell. An A:T pair contains 10 C and 7 N atoms, whereas a G:C pair contains 9 and 8, respectively. Thus, for both elements, an A:T vs. G:C exchange adds/subtracts just a single atom, changing the elemental usages of C and N by fractions of $\sim 10^{-10}$ and 0.5×10^{-9}, respectively, both of which are below the drift barrier for this species. As *E. coli* is a very high N_e species, this suggests that selection operating on elemental composition of single nucleotides is unlikely to be effective in cellular organisms.

In contrast, the maximum difference for C content among the 20 amino acids is 9 for tryptophan vs. glycine, and for N is 3 (arginine vs. several other residues). The maximum fractional impact of a single amino-acid substitution in a single-copy protein is then $\sim 10^{-9}$ for C and 5×10^{-9} for N, close to the most generous drift barrier for bacteria (Figure 1). However, most proteins are present in multiple copies per cell, so these numbers need to be multiplied accordingly. For *E. coli,* the mean number of proteins per cell is $\simeq 2000$ with a very large standard deviation ($\simeq 5000$) [8], seemingly placing the total elemental costs of some amino-acid substitutions in the realm of selective sensitivity, as the maximum impact (s_c) will commonly be in the range of 10^{-6} to 10^{-5}.

It is less clear that this will be true in eukaryotes. The number of atoms of a particular type per cell can be expected to increase roughly linearly with cell volume, but the number of proteins per cell increases with the 2/3rds power of cell volume [8]. Given these scalings, the cost/benefit of an amino-acid substitution would be expected to decline with the 2/3rds power of cell volume. Because N_e declines by two to five orders of magnitude from bacteria to eukaryotes, it appears questionable as to whether cellular elemental composition can be driven by natural selection in eukaryotes, especially in multicellular species, except perhaps in the most highly expressed genes.

Membranes and cell walls. Owing to the relatively high biosynthetic costs of lipids, membranes constitute one of the predominant costs of building cells. All cells are surrounded by a lipid bilayer, and Gram-negative bacteria have two of these sandwiching a carbohydrate-derived cell wall. Plants and some fungi also have cell walls. Because external membranes form the surface of the cell, their area scales with the $\sim 2/3$rds power of cell volume, thereby becoming proportionally less of an energy drain in larger cells. However, the emergence of eukaryotes was accompanied by the establishment of an internal-membrane system, including the nucleus, endoplasmic reticulum, Golgi, and vesicle-transport systems. Thus, it is of interest to know the degree to which the investment in internal membranes exceeds the reduction in cell-surface investment. Although a full census of internal membranes only exists for a few eukaryotes, the data suggest that these two opposing changes are roughly balanced, rendering a total contribution of lipids (internal plus external membranes) to the cell's energy budget in the range of ~ 10 to 30% across eukaryotes, which is comparable to the $\sim 20\%$ investment in cell-membrane lipids in the moderate-sized bacteria *B. subtilis* and *E. coli* ([22], see also the Supplemental Text).

These kinds of observations provide a context in which to evaluate Lane and Martin's suggestion that the origin of the mitochondrion precipitated a bioenergetics revolution necessary for the origin of eukaryotes [70]. The crux of their argument is that movement of the power-generating machine of the cell, ATP synthase, to internal membranes by-passed surface:volume ratio limitations in bacteria (where ATP synthase resides in the cell membrane). These ideas need to be tempered by the fact that mitochondrial membranes impose an investment cost equivalent to increasing the energy requirements for building a eukaryotic cell by $\sim 5\%$, and that when scaled to cell volume, the number of ribosomes and ATP-synthase complexes per eukaryotic cell are no greater than what is found in bacteria [8, 22]. These observations and others (including the progressive reduction in cell-division rate with cell volume in eukaryotes but not prokaryotes [8]) are inconsistent with the idea that the establishment of the mitochondrion spawned a bioenergetic revolution.

We now turn to the previously unexplored issue of cell walls. Although such structures provide obvious advantages

in certain ecological settings, cell walls have been lost in most eukaryotic and a few bacterial lineages, presumably during periods in which the investment in biosynthesis outweighed any fitness advantages. Indirect evidence suggests that cell walls comprise a substantial fraction of a cell's energy budget. For example, [71] estimate that $\sim 21\%$ of the biomass of a *S. cerevisiae* cell consists of the cell wall ($\sim 4\%$ protein, 30% mannose, 60% glycan, and 1% chitin). The glycan subunits are derived from $\sim 7.7 \times 10^9$ glucose molecules, which would otherwise be available for cellular energy or as carbon skeletons for other biosynthetic pathways ([72]. Similar numbers were derived for another yeast species, *Candida albicans* [72].

A more explicit statement can be made on the cost of surface layers in bacteria. Although their cell envelopes have diverse kinds of organization, bacteria can be roughly categorized into Gram-negative vs. Gram-positive classes. The Gram-negative envelope consists of an internal cell membrane, overlain by a peptidoglycan layer (the cell wall), and then by an outer membrane. In contrast, Gram-positive bacteria have thicker peptidoglycan layers and lack outer membranes. Bacterial cell envelopes have two fairly obvious roles – maintaining turgor pressure and preventing hazardous hydrophobic molecules from entering the cell, but other likely functions include attachment to environmental surfaces, and in the case of pathogens, evasion of the host's immune response by masking the surface of the cell [73]. Regardless of the perceived benefits of the various layers, to be maintained by natural selection, the advantages must at least outweigh the costs of producing the putative structure.

Owing to the complex set of constituents in the bacterial cell wall and outer membrane, the computations of costs of these layers are quite involved, but using the known biosynthetic pathways for all subunits, we outline the basic steps in the Supplemental Text. Here we focus on just the main findings. The basic carbohydrate subunit of peptidoglycan consists of two fused molecules, NAG (N-acetylglucosamine) and NAM (N-acetylmuramic acid), with short peptide chains fused to the latter for cross-bridging. Applying the methods outlined in [51] to the known pathway for peptidoglycan synthesis, the direct cost of synthesis of each peptidoglycan unit is equivalent to ~ 15 ATP hydrolyses, whereas the opportunity cost is equivalent to ~ 208 ATPs. There are $\sim 3.5 \times 10^6$ disaccharides in the entire cell wall of the Gram-negative *E. coli* [74, 75], suggesting a direct cost of $\sim 5.25 \times 10^7$ ATP hydrolyses for cell-wall biosynthesis. To put this in context, the direct cost of lipids in the cell membrane of *E. coli* is $\sim 2.5 \times 10^8$ ATPs. Although these numbers are approximate, they suggest that the fraction of a Gram-negative bacterium's energy budget associated with the cell wall is $\sim 10\times$ less than the cost of the cell membrane lipids.

Expanding this approach to the outer membrane components in *E. coli* and to the cell envelope of the Gram-positive bacterium *B. subtilis* (Supplemental Text), allows some general statements about the overall envelope costs in these two species (Figure 8). First, despite the large organizational differences and their presumed ecological consequences, both types of envelopes constitute $\sim 30\%$ of the cell's total ATP utilization, with the opportunity costs greatly exceeding the direct costs. Second, membranes are the most expensive components of the envelope in both types of bacteria. Contrary to previously reported results [22], the membrane of *B. subtilis* is costlier than that of *E. coli* owing to the former's high content of branched fatty acids (see Supplemental Text). Third, the most expensive molecular constituent of bacterial envelopes is the sugar decorations – lipopolysaccharide (2243 ATPs) in Gram-negative, and wall teichoic acid (1916 ATPs) and lipoteichoic acid (506 ATPs) in Gram-positive bacteria (Supplement Figure 2). For comparison, the average lipid costs are ~ 300 ATPs (271 in *E. coli* and 344 in *B. subtilis*). Fourth, peptidoglycan of *B. subtilis* costs more than that of *E. coli*, and this estimate is conservative given that it assumed that *B. subtilis* has only five layers.

Motility. Many cells can swim, and it is easy to imagine adaptive reasons for doing so, e.g., directive movement towards patchy resources and avoidance of predators, but not all cells living in aquatic environments can self-propel. The latter include many planktonic bacteria, diatoms, and green algae. This suggests that the energetic cost of swimming and building the mobility apparatus may exceed the benefits in certain settings.

The power requirement for swimming can be estimated as the work necessary to move an object at a particular velocity. However, the estimated costs of moving flagella indicate that the cellular conversion of chemical energy into directed swimming is universally low, averaging $\sim 2\%$ in diverse unicellular species (bacteria, archaea, ciliates, euglenoids and green algae) [76–84]. Brownian-motion jostling of cells, rotational diffusion, helical swimming patterns, and flexibility of the flagellum are among the reasons for this low efficiency. Nonetheless, it has often been suggested that the total cost of swimming is trivially small in an absolute sense, e.g., often $\leq 1\%$ of a cell's baseline energy budget [77, 85–87]. As has already been emphasized, however, what may seem small in an fractional energetic sense can be quite visible to the eyes of natural selection.

An understanding of what the cost of swimming means in evolutionary terms can be obtained from the scaling relationship between average swimming speed (v in units of μm/sec) and cell volume (V in units of μm^3) observed for a wide variety of unicellular eukaryotic species, $v \simeq 10.5V^{0.30}$ (Figure 9). Noting that the radius of a sphere is $(3V/4\pi)^{1/3}$, this implies an average swimming speed for unicellular eukaryotes of ~ 8.5/sec in units of effective cell diameters, independent of cell volume. By comparison, the peak speeds of the fastest fish (marlins and sailfish) are ~ 15 body lengths/sec.

How much energy does such activity demand? Applying Stokes' Law to the low Reynolds number situations in which microbes live, for a sphere with radius r, the power required for swimming,

$$P = 6\pi r \eta v^2 \tag{4}$$

scales with the product of the viscosity of the medium (η) and the squared swimming velocity (v^2), and to account for the inefficient conversion from cellular chemical energy to motion, this must further be divided by ~ 0.02 (noted above). Assuming spherical cells, the scaling relationship for eukaryotes in Figure 9 implies $rv^2 \simeq 68V$ μm^3/sec^2, suggesting a power scaling that is essentially isometric with respect to cell volume (because v^2 scales as $\sim V^{0.60}$ and r scales as $\sim V^{0.33}$). Noting that the viscosity of water is 10^{-2} g $\cdot$ cm^{-1} $\cdot$ sec^{-1} (assuming 20°C), after appropriate changes of units, the average power requirement of swimming is estimated to be $(64 \times 10^{-19})V$ kg $\cdot$ m^2 $\cdot$ sec^{-3}, which has equivalent units of joules/sec (here, cell volume V is in units of μm^3).

To put this in more familiar terms, note that the energy associated with the hydrolysis of one mole of ATP at physiological conditions is ~ 50 kilojoules ([88], Table 3-2). Recalling Avogadro's number of molecules per mole, the power requirement for swimming in units of ATP molecules hydrolyzed/hour is then $\sim (2.5 \times 10^5)V$. Because average basal metabolic rates also scale isometrically with cell volume, as $\sim (0.4 \times 10^9)V$ ATP hydrolyses/hour [8], this suggests a fractional energetic investment (relative to baseline metabolism) in swimming of $\sim 0.06\%$ (assuming the cell is constantly swimming), independent of cell volume. This estimate does not include the biosynthetic cost of the proteins comprising a flagellum and its basal protein parts, which in the case of an *E. coli* flagellum amounts to $\sim 3.5 \times 10^8$ ATP hydrolyses in terms of direct costs alone (Supplemental Text).

These rough calculations allow some preliminary conclusions with respect to swimming in bacteria. First, recalling from above that the ATP cost of swimming is $\sim (2.5 \times 10^5)V$ per hour for eukaryotes (and not much higher for bacteria), because the average volume of an *E. coli* cell is $V \simeq 1$ μm^3, and the cell-division time is typically no more than a few hours, almost all of the cost of swimming is associated with building rather than operating the apparatus. This conclusion is strengthened by the fact that *E. coli* cells generally harbor several flagella. Assuming a moderate cell division time of one hour and a maximum of 10 flagella per cell, the lifetime cost of swimming is $\sim (2.5 \times 10^5)$, whereas the investment in the flagellar infrastructure is $\sim 4000\times$ higher. Second, from [8], the total cost of building an *E. coli* cell is $\sim 3 \times 10^{10}$ ATP hydrolyses, implying that the bioenergetic costs of operating and building each flagellum are on the order of 0.003 and 1.2%, respectively, of the total cellular energy budget allocated to growth.

Although the structures and modes of operation of eukaryotic flagella are completely different from those in bacteria, similar calculations for eukaryotes (Supplemental Text) suggest somewhat lower total costs of swimming but roughly comparable costs of flagellar construction. For example, noting that the cellular volume of the biflagellated green alga *C. reinhardtii* is ~ 200 μm^3, and allowing for a 24-hour cell division time implies an energetic cost of swimming of $\sim 1 \times 10^9$ ATP per cell life time, whereas the total protein biosynthesis costs of flagellar construction is $\sim 21 \times 10^9$ ATP hydrolyses (for each of the two flagella). In contrast to the situation in most bacteria, eukaryotic flagella are surrounded by lipid bilayers, which in the case of each *Chlamydomonas* flagellum requires another $\sim 13 \times 10^9$ ATPs in direct biosynthetic costs. Accounting for the two flagella, the total cost of building the apparatus is then on the order of $70\times$ that of actual swimming. With the total cost of building a *C. reinhardtii* cell being equivalent to $\sim 5.4 \times 10^{12}$ ATP hydrolyses [8], the relative costs of operating and constructing the flagella are 0.02 (again, assuming swimming at a constant rate) and 1.2%, respectively.

Thus, from an evolutionary perspective, the cost of swimming constitutes a significant fraction of a cell's total energy budget. It is, therefore, no surprise that many bacteria have evolved mechanisms for selective use of flagella, expressing the necessary genes only in environments providing significant benefits [89]. Prolonged periods of silencing of flagellar genes would be expected to eventually lead to the accumulation of deactivating mutations (and complete loss of motility), and this presumably explains the absence of flagella/cilia from numerous branches in the Tree of Life.

Closing Comments

Our primary goal has been to seed the development of a formal field of evolutionary cell biology based on well-established principles in evolutionary genetics. One of the great problems in biology is the common adherence to the belief that all aspects of biodiversity have been optimized by processes of natural selection. Compelling empirical evidence suggests otherwise at the molecular and cellular levels, and the theory presented above provides a formal path to understanding the limits to what selection can accomplish in alternative population-genetic environments.

Natural selection is ubiquitous, and we are not advocating that overtly maladaptive evolution is rampant, but simply that there is ample room in the domain of effective neutrality in most species, particularly eukaryotes, that significant changes at the molecular and cellular levels are likely to accrue over long evolutionary time periods in the absence of diversifying selection. Once established, the cumulative changes in gene structure and genome architecture dictated by drift and biased mutation results in a fundamental shift in the types of real estate upon which natural selection operates via descent with modification.

The steady-state distribution approach that we present is meant to yield insight into the degree to which mean phenotypes might exhibit scaling relationships with organism size, as a consequence of the latter having side effects on the power of random genetic drift. This approach also provides a basis for understanding how mutation, even if unbiased, can push a mean phenotype away from its optimum, the more so the smaller the effective population size. Finally, the concept of haplotypic multiplicity provides a conceptual basis for understanding how species exposed to identical pressures of mutation, selection, and random genetic drift can come to harbor alternative molecular/cellular features.

Consistent with this view, accumulating evidence implies that there are often multiple degrees of freedom for accomplishing the same cellular function, post-translational modification being one such example. Others examples include: 1) the multiple layers of surveillance in replication fidelity, which are free to wander so long as the joint level of fidelity consistent with the drift barrier is maintained [90]; 2) the alternative multimeric states of homologous proteins across the Tree of Life [25]; and 3) shifts in transcription-factor binding motifs [1]. Most notable is the emergence of many examples of the evolutionary rewiring of the components of key pathways with no known change in function, including: meiosis and the cell cycle [91–93]; biosynthesis [94–98]; motility [99]; mating-type specification [100,101]; and ribosome production [102,103]. These diverse observations suggest that redundancies are common even at higher levels of organization, at least in eukaryotes, allowing for effectively neutral divergence.

The evolutionary-cost approach that we present provides a more explicit basis for understanding the granularity of the types of mutational changes that can be perceived by natural selection in different population-genetic contexts. Such analyses raise the possibility of evaluating the degree to which mildly deleterious alterations can passively accumulate by mutation pressure alone in small-N_e lineages, while being efficiently purged from species with large N_e. Likewise, it becomes possible to understand the elevated degree of evolutionary fine-tuning that can be accomplished by selection in small-N_e populations, with large-N_e populations being biased towards restricted use of large-effect adaptive mutations, which are almost certainly less frequent than the former.

The evolutionary-cost framework may also serve as a useful guide to understanding the conditions necessary for the passive emergence of cellular complexity by the process of constructive neutral evolution (CNE; [104–106]). Under this model, an ancestral cellular function is carried out by the product of a single gene (A). A fortuitous binding interaction then develops with another protein B, which initially has negligible negative effects on both A and B's functionality and on cell fitness. However, by binding to part of A's surface, B may suppress the effects of future mutations arising at the A:B interface that would otherwise compromise the stability of A. Over time, this permissive interfacial environment might lead to enough mutational buildup that A would no longer be functional in the absence of B. In principle, this evolved functional dependence of A on B could be followed by a similar scenario involving a third protein, C, and so on, imposing a sort of neutral ratchet-like mechanism towards complexity. Under this scenario, the intricate interdependencies of the large numbers of subcomponents of complexes like the ribosome and the spliceosome need not have been selected for on the basis of their intrinsic advantages, but instead could be at least in part the result of a long series of fortuitous and effectively neutral steps accompanied by the accumulation of previously forbidden mutations, which then enforces collaboration.

This verbal model for CNE illustrates the need for the kinds of quantitative analyses made possible by evolutionary-cost evaluation. One of the key assumptions of the CNE hypothesis is the existence of excess capacity within cells. This assumption is critical because the successful evolutionary diversion of B molecules to A requires that any pre-existing benefits of B are not compromised to a level that could be opposed by natural selection. As excess capacity implies a superfluous energetic drain on the ancestral cell, this raises the question as to why such a condition would

exist in the first place. Based on the theory outlined above, such a scenario would be most likely if the initial condition of excess capacity of B were effectively neutral, which is more likely with a small effective population size, consistent with the idea that small N_e facilitates the passive emergence of cellular complexity.

Finally, we note that in principle, there is no reason the general approach to estimating evolutionary costs cannot be applied to multicellular organisms, although owing to uncertainties regarding tissue-specific expression, the necessary computations will be more involved. An interesting start in this direction has been made by [107] in an analysis of the cost of signal transduction in the cell cycle of developing embryos.

Acknowledgments
This research was supported by the Multidisciplinary University Research Initiative awards W911NF-09-1-0444 and W911NF-09-1-0444 from the US Army Research Office, National Institutes of Health award R35-GM122566-01, and National Science Foundation award MCB-1518060 to ML. We thank Paul Schavemaker, Guillaume Le Treut, Ron Milo and two anonymous reviewers for helpful comments.

References

[1] M. Lynch, M. C. Field, H. Goodson, H. S. Malik, J. B. Pereira-Leal, D. S. Roos, A. Turkewitz, and S. Sazer. Evolutionary cell biology: two origins, one objective. *Proc. Natl. Acad. Sci. USA*, 111:16990–16994, 2014. doi: 10.1073/pnas.1415861111.

[2] B. Charlesworth and D. Charlesworth. *Elements of Evolutionary Genetics*. W. H. Freeman, New York, NY, 2010.

[3] J. B. Walsh and M. Lynch. *Evolution and Selection of Quantitative Traits*. Oxford Univ. Press, Oxford, UK, 2018.

[4] S. J. Gould and R. C. Lewontin. The spandrels of san marco and the panglossian paradigm: a critique of the adaptationist programme. *Proc. Royal Soc. Lond., Series B*, 205:581–598, 1979. doi: 10.1098/rspb.1979.0086.

[5] M Lynch. The frailty of adaptive hypotheses for the origins of organismal complexity. *Proc. Natl. Acad. Sci. USA*, 104 (Suppl.):8597–8604, 2011. doi: 10.1002/iub.489.

[6] M. Kimura. *The Neutral Theory of Molecular Evolution*. Cambridge Univ. Press, Cambridge, UK, 1983.

[7] M Lynch. *The Origins of Genome Architecture*. Sinauer Assocs., Inc., Sunderland, MA, 2007.

[8] M. Lynch and G. K. Marinov. The bioenergetic costs of a gene. *Proc. Natl. Acad. Sci. USA*, 112:15690–15695, 2015. doi: 10.1073/pnas.1514974112.

[9] B. Charlesworth. Effective population size and patterns of molecular evolution and variation. *Genetics*, 10:195–205, 2009. doi: 10.1038/nrg2526.

[10] T. Ohta. Slightly deleterious mutant substitutions in evolution. *Nature*, 246:96–98, 1973. doi: 10.1038/246096a0.

[11] B. Charlesworth. The effects of deleterious mutations on evolution at linked sites. *Genetics*, 190:5–22, 2012. doi: 10.1534/genetics.111.134288.

[12] R. A. Neher. Genetic draft, selective interference, and population genetics of rapid adaptation. *Ann. Rev. Ecol. Evol. Syst.*, 44:195–215, 2013. doi: 10.1146/annurev-ecolsys-110512-135920.

[13] M. Lynch, J. Blanchard, D. Houle, T. Kibota, S. Schultz, L. Vassilieva, and J. Willis. Spontaneous deleterious mutation. *Evolution*, 53:645–663, 1999. doi: 10.2307/2640707.

[14] C. F. Baer, M. M. Miyamoto, and D. R. Denver. Mutation rate variation in multicellular eukaryotes: causes and consequences. *Nat. Rev. Genet.*, 8:619–631, 2007. doi: 10.1038/nrg2158.

[15] P. D. Keightley. The distribution of mutation effects on viability in *Drosophila melanogaster*. *Genetics*, 138:1315–1322, 1994.

[16] L. Robert, J. Ollion, J. Robert, X. Song, I. Matic, and M. Elez. Mutation dynamics and fitness effects followed in single cells. *Science*, 359:1283–1286, 2018. doi: 10.1126/science.aan0797.

[17] K. B. Böndel, S. A. Kraemer, T. Samuels, D. McClean, J. Lachapelle, R. W. Ness, N. Colegrave, and P. D. Keightley. Inferring the distribution of fitness effects of spontaneous mutations in *Chlamydomonas reinhardtii*. *PLoS Biol.*, 17:e3000192, 2019. doi: 10.1371/\protect\unhbox\voidb@x\hbox{journal}.pbio.3000192.

[18] P. D. Keightley and A. Eyre-Walker. Joint inference of the distribution of fitness effects of deleterious mutations and population demography based on nucleotide polymorphism frequencies. *Genetics*, 177:2251–2261, 2007. doi: 10.1534/genetics.107.080663.

[19] T. Bataillon and S. F. Bailey. Effects of new mutations on fitness: insights from models and data. *Ann. N. Y. Acad. Sci.*, 1320:76–92, 2014. doi: 10.1111/nyas.12460.

[20] C. D. Huber, B. Y. Kim, C. D. Marsden, and K. E. Lohmueller. Determining the factors driving selective effects of new nonsynonymous mutations. *Proc. Natl. Acad. Sci. USA*, 114:4465–4470, 2015. doi: 10.1073/pnas.1619508114.

[21] B. Y. Kim, C. D. Huber, and K. E. Lohmueller. Inference of the distribution of selection coefficients for new nonsynonymous mutations using large samples. *Genetics*, 206:345–361, 2017. doi: 10.1534/genetics.116.197145.

[22] M Lynch, M. Ackerman, K. Spitze, Z. Ye, and T. Maruki. Population genomics of *Daphnia pulex*. *Genetics*, 206:315–332, 2016. doi: 10.1534/genetics.116.190611.

[23] W. Sung, M. S. Ackerman, M. Dillon, T. Platt, C. Fuqua, V. Cooper, and M. Lynch. Evolution of the insertion-deletion mutation rate across the tree of life. *G3*, 6:2583–2591, 2016. doi: 10.1534/g3.116.030890.

[24] M. Kimura. On the probability of fixation of mutant genes in a population. *Genetics*, 47:713–719, 1962.

[25] M Lynch. Evolutionary diversification of the multimeric states of proteins. *Proc. Natl. Acad. Sci. USA*, 110:E2821–E2828, 2013. doi: 10.1073/pnas.1310980110.

[26] M Lynch. Phylogenetic diversification of cell biological features. *Elife*, 7:e34820, 2018. doi: 10.7554/eLife.34820.

[27] L. Y. Yampolsky and A. Stoltzfus. Bias in the introduction of variation as an orienting factor in evolution. *Evol. Dev.*, 3:73–83, 2001. doi: 10.1046/j.1525-142x.2001.003002073.x.

[28] A. Stoltzfus and K. Cable. Mendelian-mutationism: the forgotten evolutionary synthesis. *J. Hist. Biol.*, 47:501–546, 2014. doi: 10.1007/s10739-014-9383-2.

[29] J. F. Storz, C. Natarajan, A. V. Signore, C. C. Witt, D. M. McCandlish, and A. Stoltzfus. The role of mutation bias in adaptive molecular evolution: insights from convergent changes in protein function. *Philos. Trans. R. Soc. Lond. B Biol. Sci.*, 374:20180238, 2019. doi: 10.1098/rstb.2018.0238.

[30] E. I. Svensson and D. Berger. The role of mutation bias in adaptive evolution. *Trends Ecol. Evol.*, 34:422–434, 2019. doi: 10.1016/j.tree.2019.01.015.

[31] M Lynch, M. Ackerman, J.-F. Gout, H. Long, W. Sung, W. K. Thomas, and P. L. Foster. Genetic drift, selection, and evolution of the mutation rate. *Nature Rev. Genetics*, 17:704–714, 2016. doi: 10.1038/nrg.2016.104.

[32] H. Long, W. Sung, S. Kucukyildirim, E. Williams, W. Guo, C. Patterson, C. Gregory, C. Strauss, C. Stone, C. Berne, D. Kysela, W. R. Shoemaker, M. Muscarella, H. Luo, J. T. Lennon, Y. V. Brun, and M. Lynch. Evolutionary determinants of genome-wide nucleotide composition. *Nature Ecol. Evol.*, 2:237–240, 2017. doi: 10.1038/s41559-017-0425-y.

[33] M. Kimura. On the evolutionary adjustment of spontaneous mutation rates. *Genet. Res.*, 9:23–34, 2017. doi: 10.1017/S0016672300010284.

[34] M Lynch. The cellular, developmental, and population-genetic determinants of mutation-rate evolution. *Genetics*, 180:933–943, 2008. doi: 10.1534/genetics.108.090456.

[35] M Lynch. The lower bound to the evolution of mutation rates. *Genome Biol. Evol.*, 3:1107–1118, 2011. doi: 10.1093/gbe/evr066.

[36] J. F. Gout, W. K. Thomas, Z. Smith, K. Okamoto, and M. Lynch. Large-scale detection of in vivo transcription errors. *Proc. Natl. Acad. Sci. USA*, 110:18584–18589, 2013. doi: 10.1073/pnas.1309843110.

[37] J.-F. Gout, W. Li, C. Fritsch, A. Li, S. Haroon, L. Singh, D. Hua, H. Fazelinia, S. Seeholzer, M. Lynch, and M. Vermulst. The landscape of transcription errors in eukaryotic cells. *Proc. Natl. Acad. Sci. USA*, 3:e1701484, 2017. doi: 10.1126/sciadv.1701484.

[38] C. R. Landry, E. D. Levy, and S. W. Michnick. Weak functional constraints on phosphoproteomes. *Trends Genet.*, 25(5):193–7, 2009. doi: 10.1016/j.tig.2009.03.003.

[39] A. N. Nguyen Ba and A. M. Moses. Evolution of characterized phosphorylation sites in budding yeast. *Mol. Biol. Evol.*, 27:2027–2037, 2010. doi: 10.1093/molbev/msq090.

[40] V. E. Gray and S. Kumar. Rampant purifying selection conserves positions with posttranslational modifications in human proteins. *Mol. Biol. Evol.*, 28:1565–1568, 2011. doi: 10.1093/molbev/msr013.

[41] E. D. Levy, S. W. Michnick, and C. R. Landry. Protein abundance is key to distinguish promiscuous from functional phosphorylation based on evolutionary information. *Philos. Trans. R. Soc. Lond. B Biol. Sci.*, 367:2594–2606, 2012. doi: 10.1098/rstb.2012.0078.

[42] A. M. Moses, M. E. Liku, J. J. Li, and R. Durbin. Regulatory evolution in proteins by turnover and lineage-specific changes of cyclin-dependent kinase consensus sites. *Proc. Natl. Acad. Sci. USA*, 104:17713–17718, 2007. doi: 10.1073/pnas.0700997104.

[43] L. J. Holt, B. B. Tuch, J. Villén, A. D. Johnson, S. P. Gygi, and D. O. Morgan. Global analysis of cdk1 substrate phosphorylation sites provides insights into evolution. *Science*, 325:1682–1686, 2009. doi: 10.1126/science.1172867.

[44] L. Freschi, M. Osseni, and C. R. Landry. Functional divergence and evolutionary turnover in mammalian phosphoproteomes. *PLoS Genet.*, 10(1):e1004062, 2014. doi: 10.1371/journal.pgen.1004062.

[45] et al. Studer, R. A. Evolution of protein phosphorylation across 18 fungal species. *Science*, 354:229–232, 2016. doi: 10.1126/science.aaf2144.

[46] Y. Z. Kurmangaliyev, A. Goland, and M. S. Gelfand. Evolutionary patterns of phosphorylated serines. *Biol. Direct*, 6:8, 2011. doi: 10.1186/1745-6150-6-8.

[47] S. M. Pearlman, Z. Serber, and J. E. Jr. Ferrell. A mechanism for the evolution of phosphorylation sites. *Cell*, 147:934–946, 2011. doi: 10.1016/j.cell.2011.08.052.

[48] G. Diss, L. Freschi, and C. R. Landry. Where do phosphosites come from and where do they go after gene duplication? *Int. J. Evol. Biol.*, 2012:843167, 2012. doi: 10.1155/2012/843167.

[49] G. E. Lienhard. Non-functional phosphorylations? *Trends Biochem. Sci.*, 33:351–352, 2008. doi: 10.1016/j.tibs.2008.05.004.

[50] C. R. Landry, L. Freschi, T. Zarin, and A. M. Moses. Turnover of protein phosphorylation evolving under stabilizing selection. *Front. Genet.*, 5:245, 2014. doi: 10.3389/fgene.2014.00245.

[51] G. Mahmoudabadi, M. Phillips, R. Lynch, and R. Milo. Defining the energetic costs of cellular structures. *bioRxiv*, 6, 2019. www.biorxiv.org/content/10.1101/666040v1.

[52] T. Bauchop and S. R. Elsden. The growth of micro-organisms in relation to their energy supply. *J. Gen. Microbiol.*, 23:457–469, 1960. doi: 10.1099/00221287-23-3-457.

[53] D. E. Atkinson. Adenine nucleotides as universal stoichiometric metabolic coupling agents. *Adv. Enzyme Regul.*, 9:207–219, 1970. doi: 10.1016/S0065-2571(71)80045-6.

[54] A. H. Stouthamer. A theoretical study on the amount of atp required for synthesis of microbial cell material. *Antonie Van Leeuwenhoek*, 39:545–65, 1973. doi: 10.1007/BF02578899.

[55] D. W. Tempest and O. M. Neijssel. The status of yatp and maintenance energy as biologically interpretable phenomena. *Annu. Rev. Microbiol.*, 38:459–486, 1984. doi: 10.1146/annurev.mi.38.100184.002331.

[56] J. B. Russell and G. M. Cook. Energetics of bacterial growth: balance of anabolic and catabolic reactions. *Microbiol. Rev.*, 59:48–62, 1995.

[57] M. S. Kharasch and B. Sher. The electronic conception of valence and heats of combustion of organic compounds. *J. Phys. Chem.*, 29:625–658, 1925. doi: 10.1021/j150252a001UT.

[58] C. L. Craig and R. S. Weber. Selection costs of amino acid substitutions in cole 1 and colia gene clusters harbored by *Escherichia coli*. *Mol. Biol. Evol.*, 15:774–776, 1998. doi: 10.1093/oxfordjournals.molbev.a025981.

[59] H. Akashi and T. Gojobori. Metabolic efficiency and amino acid composition in the proteomes of *Escherichia coli* and *Bacillus subtilis*. *Proc. Natl. Acad. Sci. U. S. A.*, 99:3695–3700, 2002. doi: 10.1073/pnas.062526999.

[60] E. Ilker and M. Hinczewski. Modeling the growth of organisms validates a general relation between metabolic costs and natural selection. *Phys. Rev. Lett.*, 122:238101, 2019. doi: 10.1103/PhysRevLett.122.238101.

[61] S. J. Pirt. Maintenance energy: a general model for energy-limited and energy-sufficient growth. *Arch. Microbiol.*, 133:300–302, 1982. doi: 10.1007/BF00521294.

[62] D. Molenaar, R. Van Berlo, D. De Ridder, and B. Teusink. Shifts in growth strategies reflect tradeoffs in cellular economics. *Mol. Syst. Biol.*, 5(1):1099–1102, 2009. doi: 10.1126/science.1192588.

[63] M. Scott, C. W. Gunderson, E. M. Mateescu, Z. Zhang, and T. Hwa. Interdependence of cell growth and gene expression: origins and consequences. *Science*, 330(6007):1099–1102, 2010. doi: 10.1126/science.1192588.

[64] A.Y. Weiße, D.A. Oyarzú n, V. Danos, and P.S. Swain. Mechanistic links between cellular trade-offs, gene expression, and growth. *Proc Natl Acad Sci USA.*, 112(9):pp.E1038–E1047, 2015. doi: 10.1073/pnas.1416533112.

[65] P. P. Pandey and S. Jain. Analytic derivation of bacterial growth laws from a simple model of intracellular chemical dynamics. *Theory Biosci.*, 135(3):121–130, 2016. doi: 10.1007/s12064-016-0227-9.

[66] P. Baudouin-Cornu, Y. Surdin-Kerjan, P. Marliere, and D Thomas. Molecular evolution of protein atomic composition. *Science*, 293(5528):297–300, 2001. doi: 10.1126/science.1061052.

[67] R. Alves and M.A. Savageau. Evidence of selection for low cognate amino acid bias in amino acid biosynthetic enzymes. *Mol. Microbiol.*, 56(4):1017–34, 2005. doi: 10.1111/j.1365-2958.2005.04566.x.

[68] C. Acquisti, S. Kumar, and J. J. Elser. Signatures of nitrogen limitation in the elemental composition of the proteins involved in the metabolic apparatus. *Proc. Biol. Sci.*, 276(1667):2605–2610, 2009. doi: 10.1126/science.1061052.

[69] J. P. Folsom and R. P. Carlson. Physiological, biomass elemental composition and proteomic analyses of *Escherichia coli* ammonium-limited chemostat growth, and comparison with iron- and glucose-limited chemostat growth. *Microbiology*, 161:1659–1670, 2015. doi: 10.1099/mic.0.000118.

[70] N. Lane and W Martin. The energetics of genome complexity. *Nature*, 467(7318):929–34, 2010. doi: 10.1038/nature09486.

[71] Q. Y. Yin, P. W. de Groot, L. de Jong, F. M. Klis, and C. G. De Koster. Mass spectrometric quantitation of covalently bound cell wall proteins in *Saccharomyces cerevisiae*. *FEMS Yeast Res.*, 7:887–896, 2007. doi: 10.1111/j.1567-1364.2007.00272.x.

[72] F. M. Klis, C. G. de Koster, and S. Brul. Cell wall-related bionumbers and bioestimates of *Saccharomyces cerevisiae* and *Candida albicans*. *Eukaryot. Cell*, 13:2–9, 2014. doi: 10.1128/EC.00250-13.

[73] F.C. Neidhardt, J.L. Ingraham, and M. Schaechter. *Physiology of the bacterial cell: a molecular approach*. Sunderland, MA: Sinauer Associates, 1990.

[74] F.B. Wientjes, C.L. Woldringh, and N. Nanninga. Amount of peptidoglycan in cell walls of gram-negative bacteria. *J. Bacteriol.*, 173:7684–7691, 1991. doi: 10.1128/jb.173.23.7684-7691.1991.

[75] J. C. Gumbart, M. Beeby, G. J. Jensen, and B. Roux. *Escherichia coli* peptidoglycan structure and mechanics as predicted by atomic-scale simulations. *PLoS Comput. Biol.*, 10:e1003475, 2014. doi: 10.1371/journal.pcbi.1003475.

[76] S. M. Gittleson and R. M. Noble. Locomotion in *Polytomella agilis* and *Polytoma uvella*. *Trans. Amer. Micro. Soc.*, 92:122–128, 1973. doi: 10.2307/3225176.

[77] E. M. Purcell. Life at low reynolds number. *Amer. J. Physics*, 45:3–11, 1977. doi: 10.1119/1.10903.

[78] M. Meister, G. Lowe, and H. C. Berg. The proton flux through the bacterial flagellar motor. *Cell*, 49:643–650, 1987. doi: 10.1016/0092-8674(87)90540-x.

[79] S. Chattopadhyay, R. Moldovan, C. Yeung, and X. L. Wu. Swimming efficiency of bacterium *Escherichia coli*. *Proc. Natl. Acad. Sci. USA*, 103:13712–13717, 2006. doi: 10.1073/pnas.0602043103.

[80] Y. Katsu-Kimura, F. Nakaya, S. A. Baba, and Y. Mogami. Substantial energy expenditure for locomotion in ciliates verified by means of simultaneous measurement of oxygen consumption rate and swimming speed. *J. Exp. Biol.*, 212:1819–1824, 2009. doi: 10.1242/jeb.028894.

[81] D. Tam and A. E. Hosoi. Optimal feeding and swimming gaits of biflagellated organisms. *Proc. Natl. Acad. Sci. USA*, 108:1001–1006, 2011. doi: 10.1073/pnas.1011185108.

[82] M. Arroyo, L. Heltai, D. Millán, and A. DeSimone. Reverse engineering the euglenoid movement. *Proc. Natl. Acad. Sci. USA*, 109:17874–17879, 2012. doi: 10.1073/pnas.1213977109.

[83] L. Barsanti, P. Coltelli, V. Evangelista, A. M. Frassanito, and P. Gualtieri. Swimming patterns of the quadriflagellate *Tetraflagellochloris mauritanica* (chlamydomonadales, chlorophyceae). *J. Phycol.*, 52:209–218, 2016. doi: 10.1111/jpy.12384.

[84] Y. Kinosita, N. Uchida, D. Nakane, and T. Nishizaka. Direct observation of rotation and steps of the archaellum in the swimming halophilic archaeon *Halobacterium salinarum*. *Nat. Microbiol.*, 1:16148, 2016. doi: 10.1038/nmicrobiol.2016.148.

[85] T. Fenchel and B. J. Finlay. Respiration rates in heterotrophic, free-living protozoa. *Microb. Ecol.*, 9:99–122, 1983. doi: 10.1007/BF02015125.

[86] J. A. Raven and K. Richardson. Dinophyte flagella: a cost-benefit analysis. *New Phytol.*, 98:259–276, 1984. doi: 10.1111/j.1469-8137.1984.tb02736.x.

[87] D. W. Crawford. Metabolic cost of motility in planktonic protists: theoretical considerations on size scaling and swimming speed. *Microb. Ecol.*, 24:1–10, 1992. doi: 10.1007/BF00171966.

[88] R. Milo and R. Phillips. *Cell biology by the numbers*. Garland Science, New York, NY, 2016.

[89] J. L. Ferreira, F. Z. Gao, F. M. Rossmann, A. Nans, S. Brenzinger, ... Hosseini, R., and M. Beeby. Gammaproteobacteria eject their polar flagella under nutrient depletion, retaining flagellar motor relic structures. *PLoS Biol.*, 17(3):e3000165, 2019. doi: 10.1371/\journal.pbio.3000165.

[90] M Lynch. Evolutionary layering and the limits to cellular perfection. *Proc. Natl. Acad. Sci. USA*, 109:18851–18856, 2011. doi: 10.1073/pnas.1216130109.

[91] F. R. Cross, N. E. Buchler, and J. M. Skotheim. Evolution of networks and sequences in eukaryotic cell cycle control. *Philos. Trans. R. Soc. Lond. B Biol. Sci.*, 366:3532–3544, 2011. doi: 10.1098/rstb.2011.0078.

[92] H. Harashima, N. Dissmeyer, and A. Schnittger. Cell cycle control across the eukaryotic kingdom. *Trends Cell Biol.*, 23:345–356, 2013. doi: 10.1016/j.tcb.2013.03.002.

[93] K. P. Kohl and J. Sekelsky. Meiotic and mitotic recombination in meiosis. *Genetics*, 194:327–334, 2013. doi: 10.1534/genetics.113.150581.

[94] R. A. Jensen and D. L. Pierson. Evolutionary implications of different types of microbial enzymology for l-tyrosine biosynthesis. *Nature*, 254:667–671, 2019. doi: 10.1038/254667a0.

[95] E. V. Koonin, A. R. Mushegian, and P. Bork. Non-orthologous gene displacement. *Trends Genet.*, 12:334–336, 1996. doi: 10.1016/S0168-9525(96)80003-5.

[96] H. Barreteau, A. Kovac, A. Boniface, M. Sova, S. Gobec, and D. Blanot. Cytoplasmic steps of peptidoglycan biosynthesis. *FEMS Microbiol. Rev.*, 32:168–207, 2008. doi: 10.1111/j.1574-6976.2008.00104.x.

[97] M. V. Omelchenko, M. Y. Galperin, Y. I. Wolf, and E. V. Koonin. Non-homologous isofunctional enzymes: a systematic analysis of alternative solutions in enzyme evolution. *Biol. Direct*, 5:51, 2010. doi: 10.1186/1745-6150-5-31.

[98] N. A. Liapounova, V. Hampl, P. M. K. Gordon, C. W. Sensen, L. Gedamu, and J. B. Dacks. Reconstructing the mosaic glycolytic pathway of the anaerobic eukaryote monocercomonoides. *Eukaryot. Cell*, 5:2138–2146, 2012. doi: 10.1128/EC.00258-06.

[99] T. B. Taylor, G. Mulley, A. H. Dills, A. S. Alsohim, L. J. McGuffin, D. J. Studholme, M. W. Silby, M. A. Brockhurst, L. J. Johnson, and R. W. Jackson. Evolutionary resurrection of flagellar motility via rewiring of the nitrogen regulation system. *Science*, 347:1014–1017, 2015. doi: 10.1126/science.1259145.

[100] C. R. Baker, B. B. Tuch, and A. D. Johnson. Extensive dna-binding specificity divergence of a conserved transcription regulator. *Proc. Natl. Acad. Sci. USA*, 108:7493–7498, 2011. doi: 10.1073/pnas.1019177108.

[101] D. P. Singh et al. Genome-defence small rnas exapted for epigenetic mating-type inheritance. *Nature*, 509:447–452, 2014. doi: 10.1038/nature13318.

[102] A. Tanay, A. Regev, and R. Shamir. Conservation and evolvability in regulatory networks: the evolution of ribosomal regulation in yeast. *Proc. Natl. Acad. Sci. USA*, 102:7203–7208, 2005. doi: 10.1073/pnas.0502521102.

[103] H. Lavoie, H. Hogues, J. Mallick, A. Sellam, A. Nantel, and M. Whiteway. Evolutionary tinkering with conserved components of a transcriptional regulatory network. *PLoS Biol.*, 8:e1000329, 2010. doi: 10.1371/journal.pbio.1000329.

[104] A. Stoltzfus. On the possibility of constructive neutral evolution. *J. Mol. Evol.*, 49:169–181, 1999. doi: 10.1007/PL00006540.

[105] M. W. Gray, J. Lukes, J. M. Archibald, P. J. Keeling, and W. F. Doolittle. Cell biology. irremediable complexity? *Science*, 330:920–921, 2010. doi: 10.1126/science.1198594.

[106] J. Lukes, J. M. Archibald, P. J. Keeling, W. F. Doolittle, and Gray M. W. How a neutral evolutionary ratchet can build cellular complexity. *IUBMB Life*, 63:528–537, 2011. doi: 10.1002/iub.489.

[107] J. Rodenfels, K. M. Neugebauer, and J. Howard. Heat oscillations driven by the embryonic cell cycle reveal the energetic costs of signaling. *Dev. cell*, 48(5):646–658, 2019. doi: 10.1016/j.devcel.2018.12.024.

Figure 1. The negative scaling of effective population size (N_e) with organism size across the Tree of Life. The shaded squares envelope the full range of estimated variation for each major group, and it is plausible that over evolutionary time the mutation rates of individual taxa wander between the upper and lower limits of each group, as there is drift around the drift barrier [35]. The line is the least-squares fit to the overall data $N_e = (5.1 \times 10^6)B^{-0.21}$, $r^2 = 0.87$. where B is adult dry weight (in μg). See Supplemental Table 1 for further information on sources of data.

Figure 2. Schematic for the evolutionary transition rates between adjacent genotypic classes under the sequential-fixation model for the case of $\ell = 4$ contributing genetic loci. Note that for all but the end states, there are multiple phenotypically equivalent haplotypes (with the red boxes), the number of which (the multiplicity) is defined by the coefficient of the binomial distribution. The net mutation rates between genotypic states are functions of the forward and reverse mutation rates (μ_{01} and μ_{10}) and the number of parental + and − alleles; the population size also influences the absolute flux rate, but as this is assumed to be constant, it influences all rates equally and has no influence on the final equilibrium distribution, and so is dropped from the figure. The quantities ϕ_{01} and ϕ_{10} are the probabilities of fixation of newly arising mutations, which are functions of the selective advantage of mutant relative to ancestral allele and of the absolute and genetic effective population sizes. This schematic readily generalizes to any value of ℓ.

Figure 3. An example of the response of the steady-state mean-phenotype distribution to effective population size differences with $\ell = 100$. Here fitness of genotypic class m is equal to $\exp\{-0.5[(m - 100)/20000]^2\}$, a half Gaussian such that the optimal fitness occurs for $m = 100$, and mutation is biased in the downward direction such that $u_{01} = u_{10}/25$. Selection here is weak, and distributed over $\ell = 100$ loci, with $m = 91$ having a reduction in fitness of 10^{-7}, and $m = 0$ having a reduction of 1.25×10^{-5}, so that the distribution with $N_e = 10^5$ is close to the neutral expectation (given by the left-most dashed distribution). Results are given for N_e ranging from $10^{5.5}$ to 10^9.

Figure 4. Negative scaling of the base-substitution mutation rate per nucleotide site with the effective population size. Individual regression lines, and shaded squares encompassing the data, are given for three groups of organisms. The data are primarily drawn from the compilations in [31] and [32], with a few additions that have emerged since those publications (Supplemental Table 1).

Figure 5. Growth yields per unit carbon consumed as a function of the heats of combustion of the carbon substrate (which also serves as the source of energy). The scaling follows a power-law relationship $Y = 0.042H_C^{1.47}$ ($r^2 = 0.81$) up to $H_C \simeq 10$, and thereafter levels off at a constant value $\simeq 1.3$ (units are defined in the axis labels). Results are taken from various sources in the literature (Supplemental Table 2); all results for eukaryotes involve fungi (mostly yeasts). The dashed-line threshold is fitted by eye.

Figure 6. The distinction between direct and opportunity costs associated with synthesizing monomeric building blocks. These costs are only evaluated at the point where a precursor molecule is first exploited in the biosynthetic pathway, as any earlier processing (and either gain or loss of energy) would occur regardless of the downstream modes of precursor utilization. The direct cost represents the basic biochemical expenditures involved in producing the monomeric building block, which must be taken out of the cell's total energy budget. When a precursor molecule has been utilized, the opportunity cost represents the degree to which this loss robs the cell of energy that could be used in other processes. The cost of an entire trait further entails costs of processing, assembling, and maintaining the structure derived from the underlying monomeric components.

Figure 7. The net selective advantage (disadvantage) of a cellular feature is a function of the organism's ecological context, which defines s_{direct}, and the investment cost in constructing and maintaining the trait s_{cost}. The sign and magnitude of $s_{\rm net} = s_{direct} - s_{cost}$, relative to the drift barrier, determines whether the feature will be promoted by positive selection or subject to removal by deactivating mutations.

Figure 8. Percentages of the total energy pool invested in the production of a particular envelope component. Each color signifies the total cost of a particular envelope component. Each slice with the lighter coloration represent the direct cost fraction of the correspondigly colored envelope component. "Cell budget remainder" refers to all remaining cellular processes and structures not involved in envelope production. See Supplemental Text for calculation details.

Figure 9. Scaling relationships between swimming velocities (v) and cell volume (V) in unicellular species. For eukaryotes, $v = 10.5V^{0.30}$ ($r^2 = 0.49$); and for bacteria, $v = 27.8V^{0.19}$ ($r^2 = 0.21$). The measured values are corrected

for temperature assuming a Q10 of 2.0. See Supplemental Table 3 for data and their sources.

Figure 1

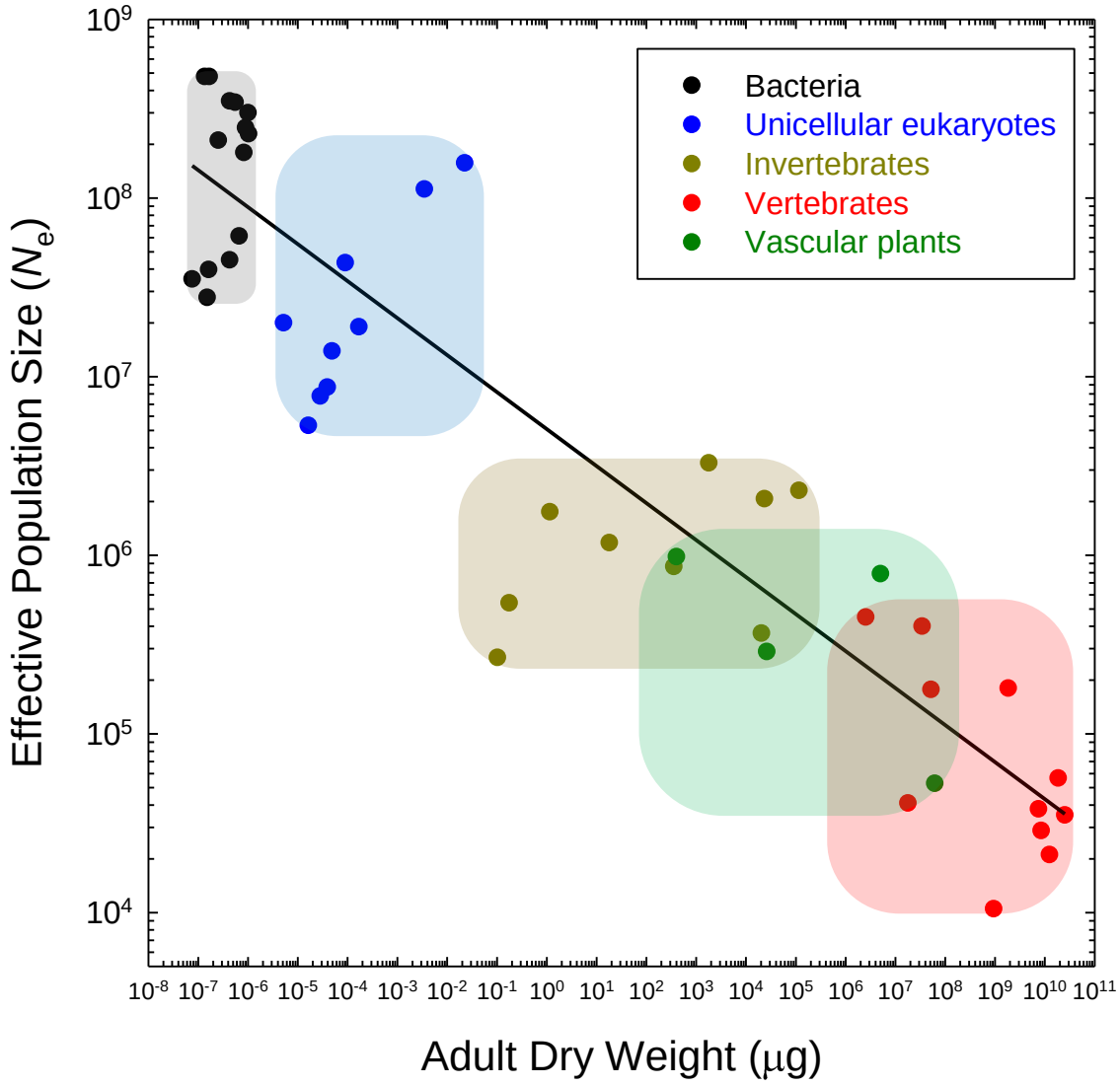
Bacteria
Unicellular eukaryotes
Invertebrates
Vertebrates
Vascular plants
Effective Population Size (N_e)
10^9
10^8
10^7
10^6
10^5
10^4
10^{-8} 10^{-7} 10^{-6} 10^{-5} 10^{-4} 10^{-3} 10^{-2} 10^{-1} 10^0 10^1 10^2 10^3 10^4 10^5 10^6 10^7 10^8 10^9 10^{10} 10^{11}
Adult Dry Weight (μg)

Figure 2

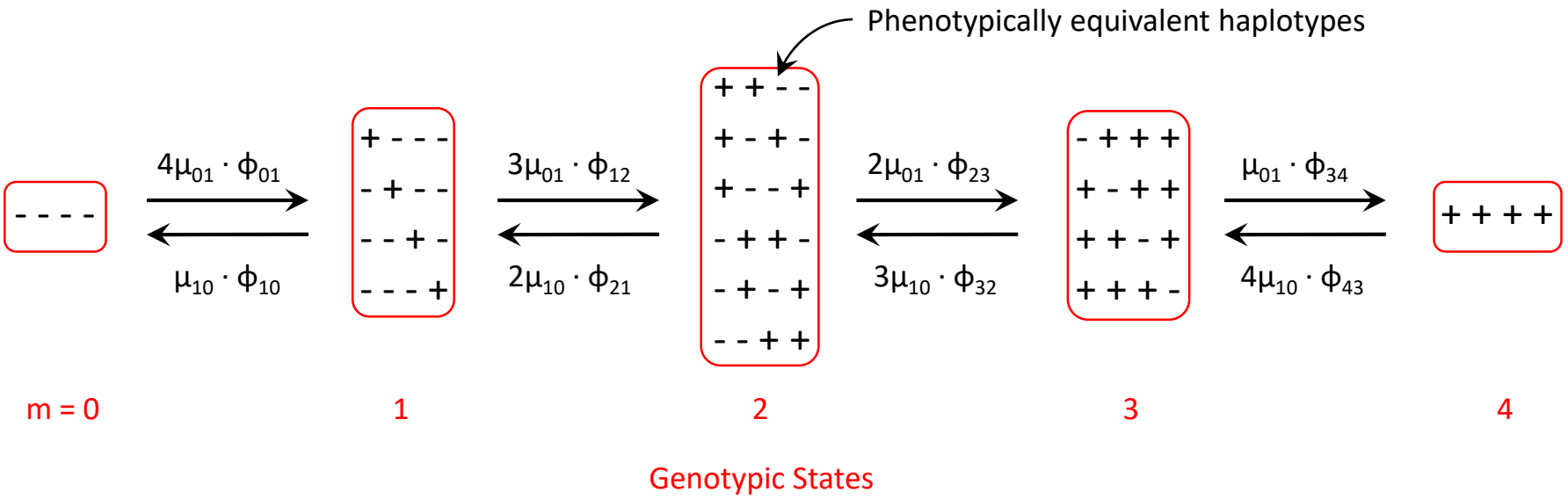
Phenotypically equivalent haplotypes
- - - -
4μ01 · ϕ01
μ10 · ϕ10
+ - - -
- + - -
- - + -
- - - +
3μ01 · ϕ12
2μ10 · ϕ21
+ + - -
+ - + -
+ - - +
- + + -
- + - +
- - + +
2μ01 · ϕ23
3μ10 · ϕ32
- + + +
+ - + +
+ + - +
+ + + -
μ01 · ϕ34
4μ10 · ϕ43
+ + + +
m = 0
1
2
3
4
Genotypic States

Figure 3

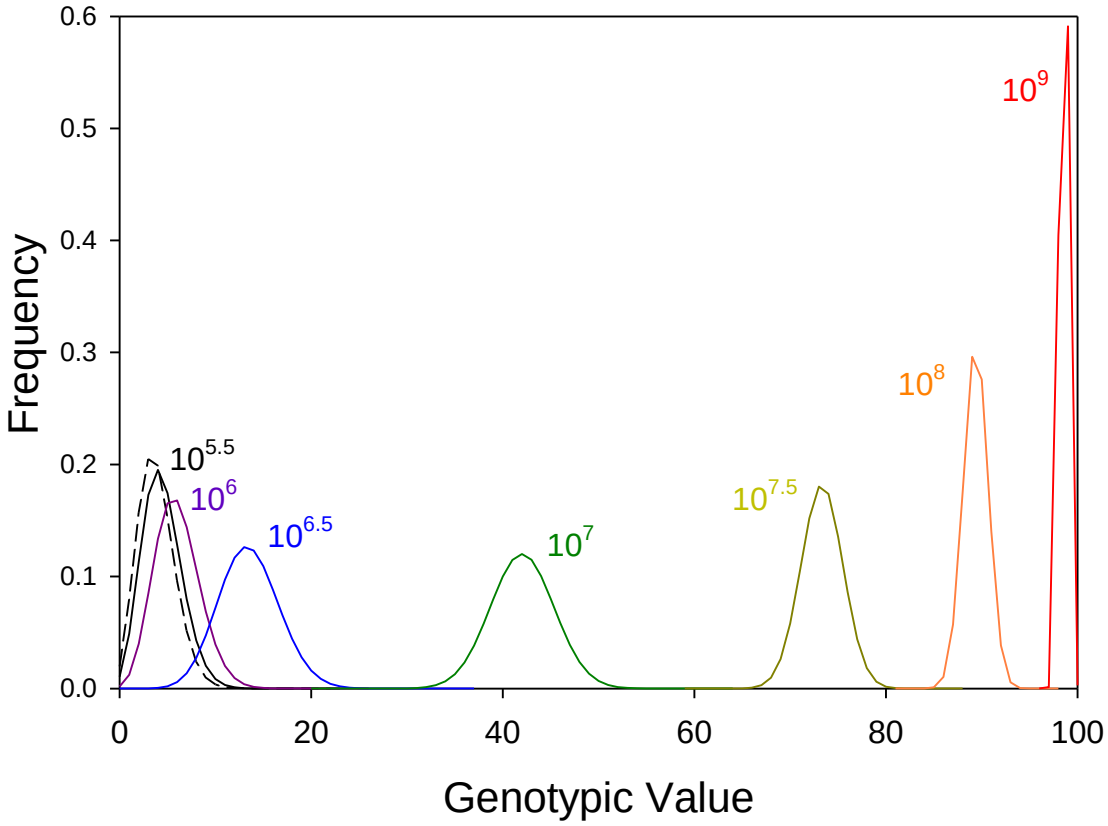
0.6
0.5
0.4
0.3
0.2
0.1
0.0
Frequency
0
20
40
60
80
100
Genotypic Value
$10^{5.5}$
10^{6}
$10^{6.5}$
10^{7}
$10^{7.5}$
10^{8}
10^{9}

Figure 4

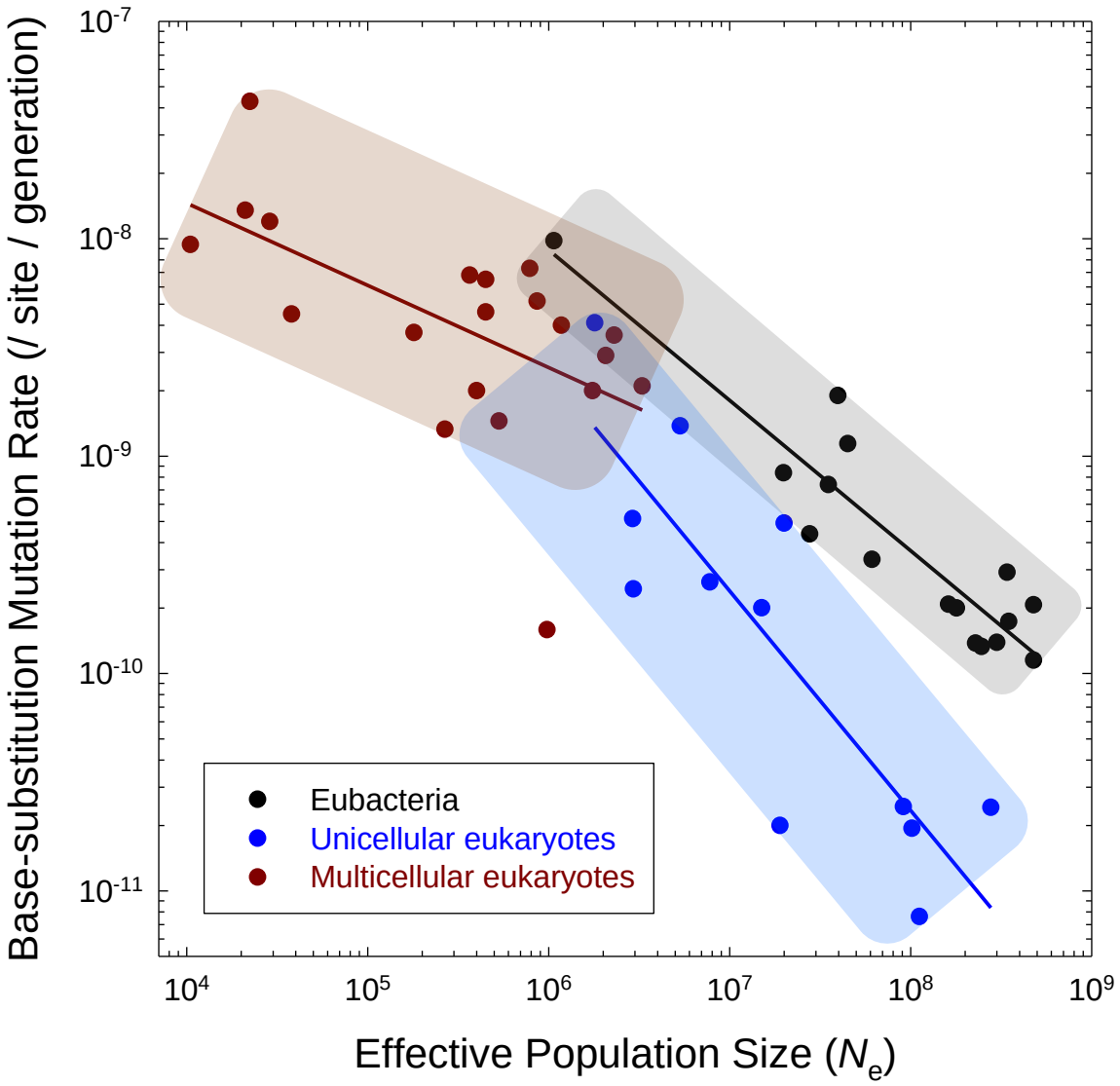
Base-substitution Mutation Rate (/ site / generation)
10-7
10-8
10-9
10-10
10-11
Eubacteria
Unicellular eukaryotes
Multicellular eukaryotes
10^4
10^5
10^6
10^7
10^8
10^9
Effective Population Size (Ne)

Figure 5

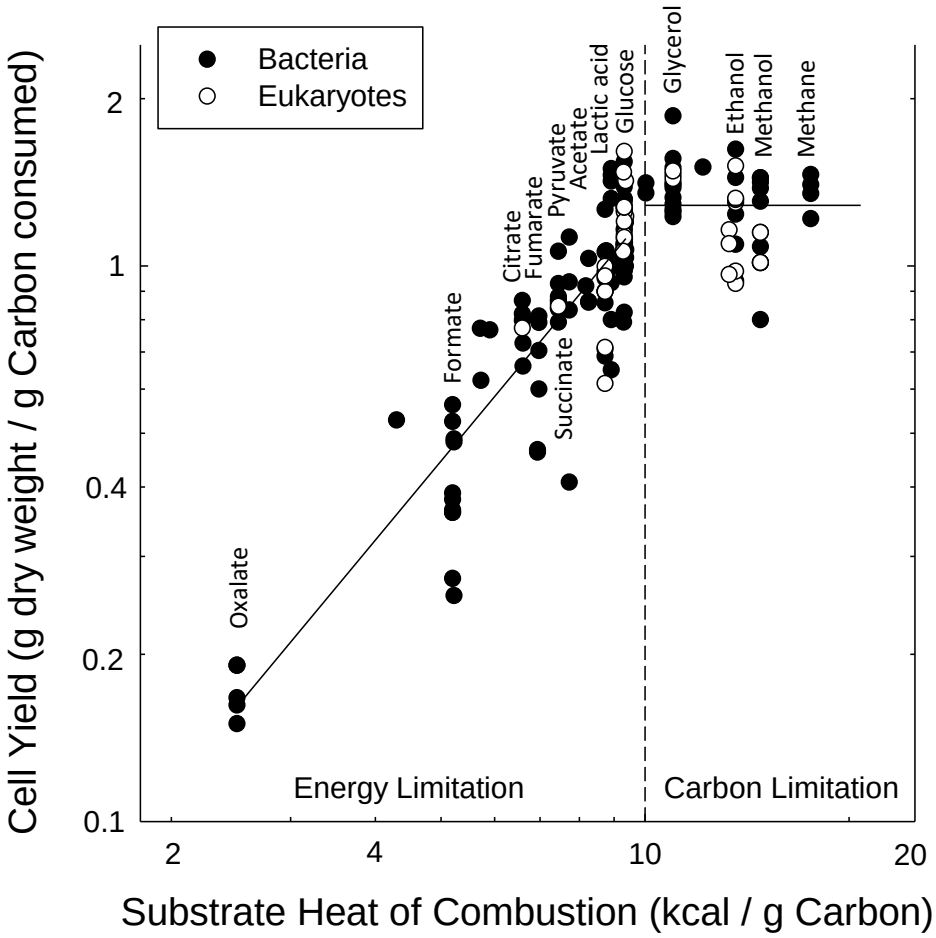
Bacteria
Eukaryotes
Oxalate
Formate
Succinate
Fumarate
Citrate
Pyruvate
Acetate
Lactic acid
Glucose
Glycerol
Ethanol
Methanol
Methane
Energy Limitation
Carbon Limitation
Cell Yield (g dry weight / g Carbon consumed)
Substrate Heat of Combustion (kcal / g Carbon)
0.1
0.2
0.4
1
2
2
4
10
20

Figure 6

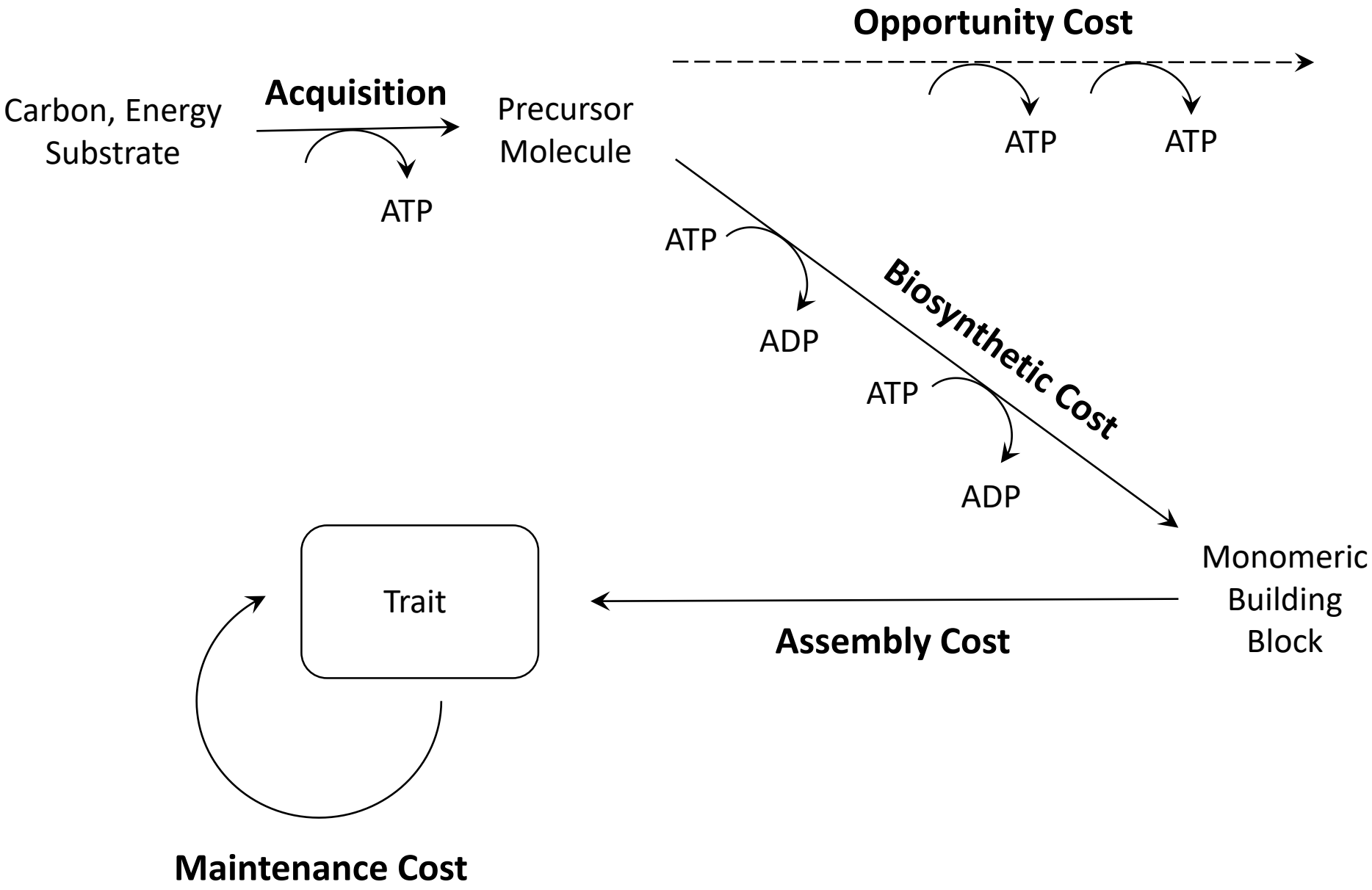
Opportunity Cost
Carbon, Energy Substrate
Acquisition
Precursor Molecule
ATP
ATP
ATP
ATP
ATP
ADP
Biosynthetic Cost
ATP
ADP
Trait
Monomeric Building Block
Assembly Cost
Maintenance Cost

Figure 7

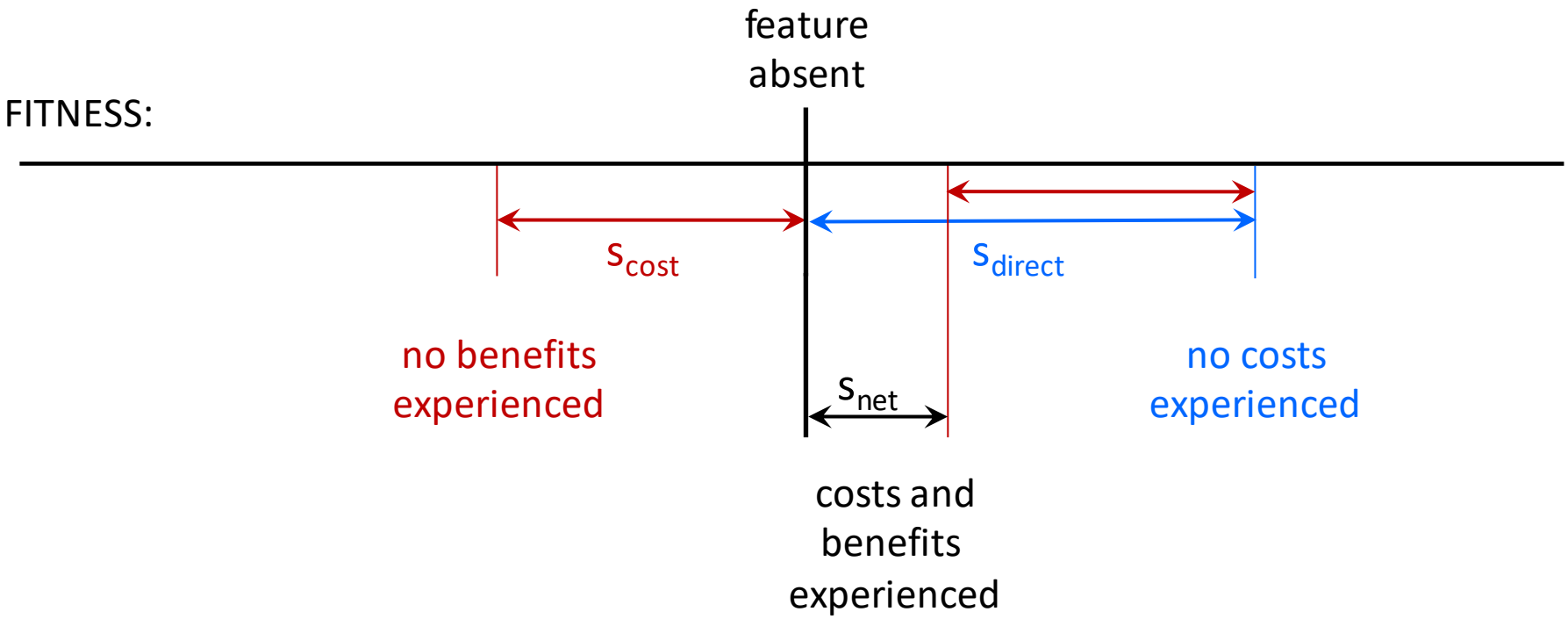
feature
absent
FITNESS:
s_{cost}
s_{direct}
no benefits
experienced
s_{net}
no costs
experienced
costs and
benefits
experienced

Figure 8

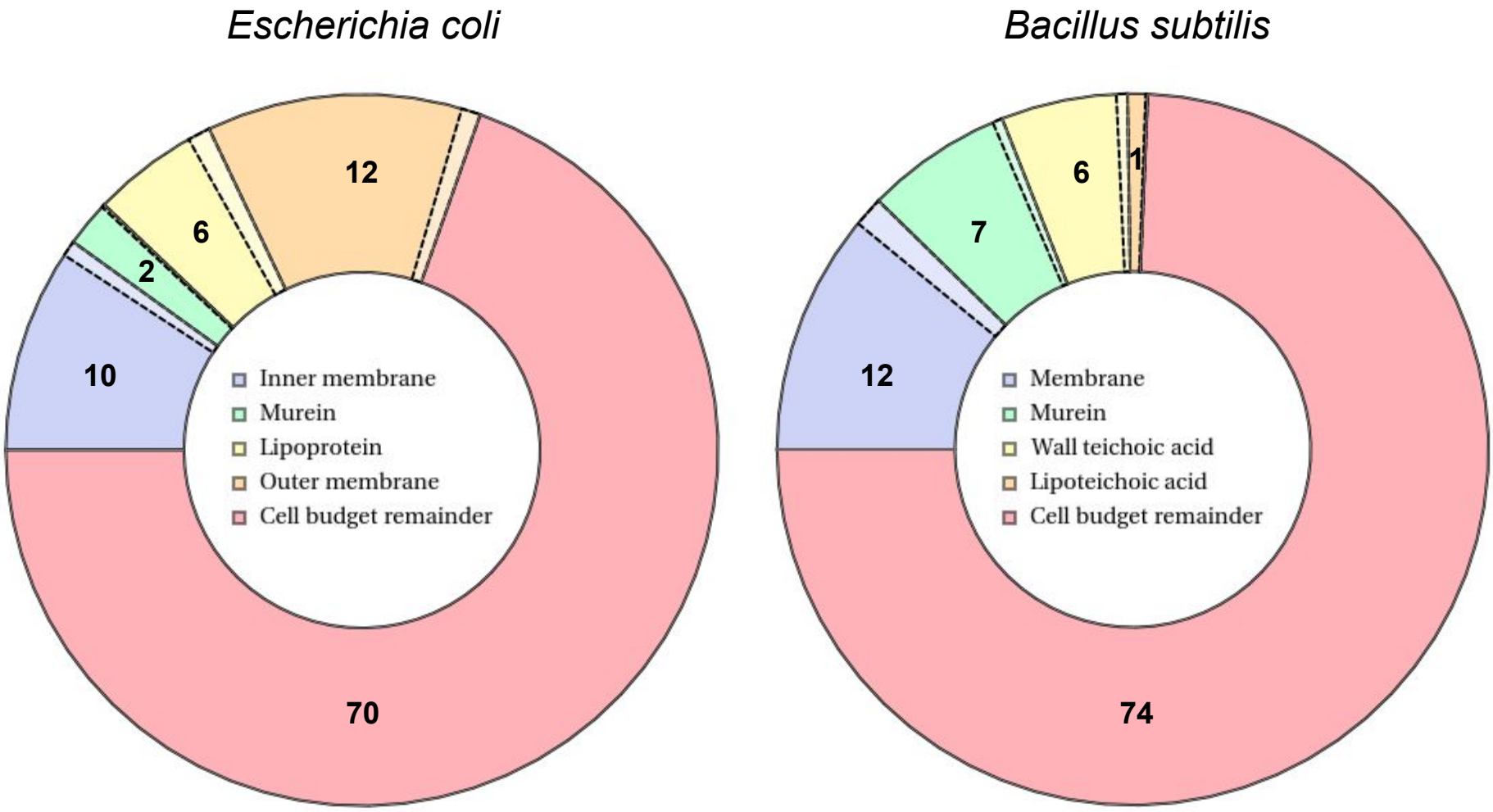
Escherichia coli
12
6
2
10
70
Inner membrane
Murein
Lipoprotein
Outer membrane
Cell budget remainder
Bacillus subtilis
6
1
7
12
74
Membrane
Murein
Wall teichoic acid
Lipoteichoic acid
Cell budget remainder

Figure 9

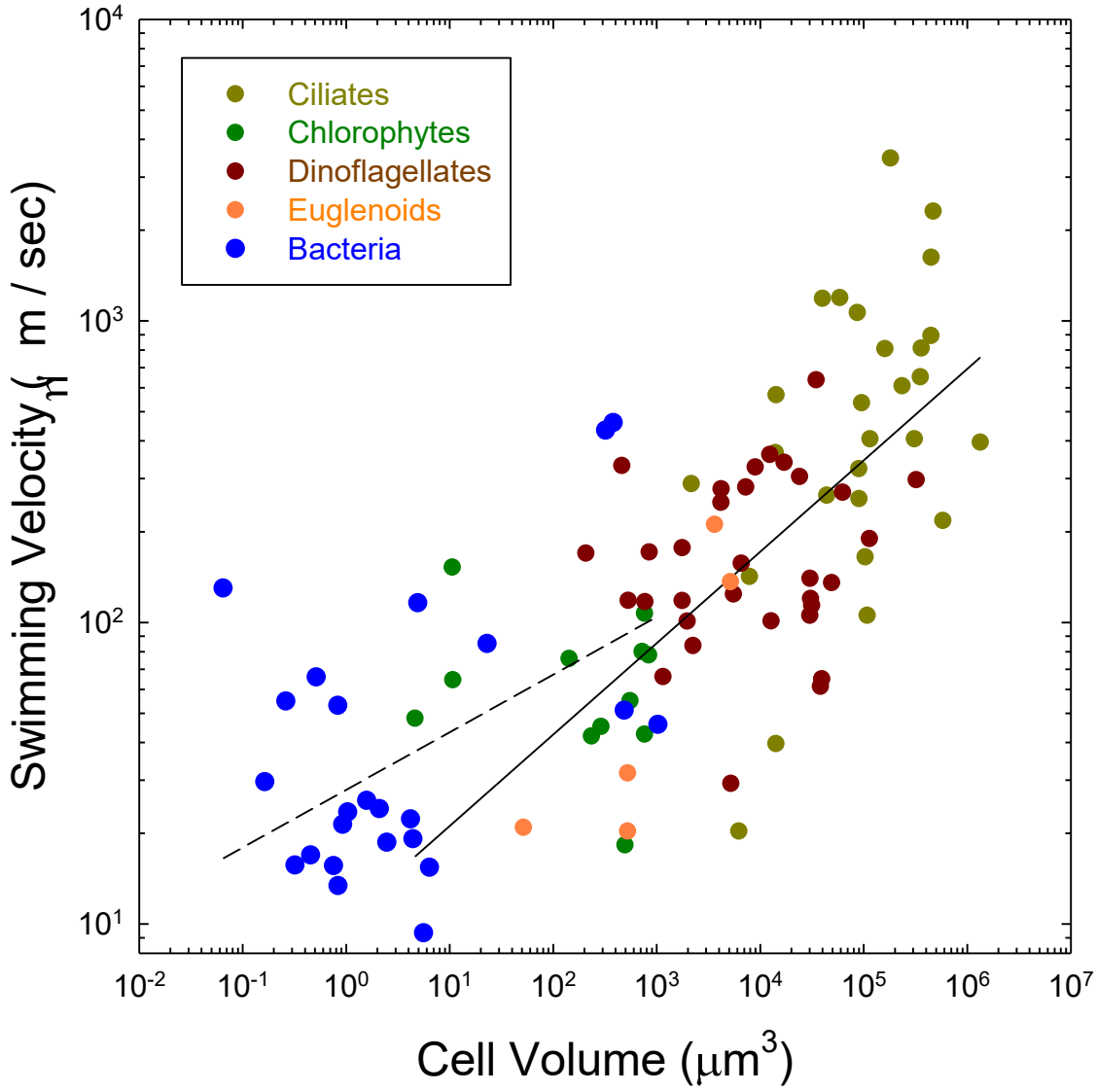
Ciliates
Chlorophytes
Dinoflagellates
Euglenoids
Bacteria
Swimming Velocity (μm / sec)
Cell Volume (μm3)
10^4
10^3
10^2
10^1
10^-2
10^-1
10^0
10^1
10^2
10^3
10^4
10^5
10^6
10^7

1. Natural selection is not an all-powerful mechanism, and other evolutionary mechanisms (genetic drift and mutation) affect the stationary distribution of the trait value. Thus, evolution cannot be always treated as an optimization process.
2. For a trait to evolve, the benefit that it confers to an individual must outweigh the cost of the trait. This holds for any trait, ranging from nutrient intake and motility, to signal sensing and cell wall. The costs are defined in terms of the amount of ATP that has to be consumed for the production and maintenance of the trait.
3. While the previous studies focused on the cost of the gene, we extend this approach to the costs of common cellular features; Namely, bacterial motility and cell envelope.